IS-T 1794

Fundamental Studies of Supported Bimetallic Catalysts by NMR Spectroscopy

by

Savargaonkar, Nilesh

PHD Thesis submitted to Iowa State University

Ames Laboratory, U.S. DOE

Iowa State University

Ames, Iowa 50011

Date Transmitted: October 17, 1996

PREPARED FOR THE U.S. DEPARTMENT OF ENERGY

UNDER CONTRACT NO. W-7405-Eng-82.

DISCLAIMER

DEDICATION

To my mother, Usha Savargaonkar and father, Ramakant Savargaonkar who inspired me to reach higher goals and gave me moral support to struggle for achieving my goals

TABLE OF CONTENTS

Preprint — to be processed separately

Preprint — to be processed separately

Preprint — to be processed separately

Preprint — to be processed separately

Preprint - to be processed separately

ABSTRACT

Characterization of a bimetallic catalyst in terms of its surface composition is important in understanding the mechanisms of reactions over such catalysts. Since catalytic surfaces are covered with adsorbates under reaction conditions, the influence of adsorbates on the surface compositions of bimetallic catalysts is also important. Hydrogen was found to influence the surface compositions of silica and alumina supported Pt-Rh catalysts to a certain extent as the surfaces of bimetallic catalysts were enriched in Rh under the influence of hydrogen. Although the extent of Rh enrichment of the surface was not large, the surface compositions in the presence of hydrogen were significantly different from those of an adsorbate-free Pt-Rh surface which is known to be enriched in Pt.

Various hydrogenation reactions on transition metals are important commercially whereas certain hydrogenolysis reactions are useful from fundamental point of view. Understanding the hydrogen mobility and kinetics of adsorption-desorption of hydrogen is important in understanding the mechanisms of such reactions involving hydrogen. The kinetics of hydrogen chemisorption was studied by means of selective excitation NMR on silica supported Pt, Rh and Pt-Rh catalysts. The activation energy of hydrogen desorption was found to be lower on silica supported Pt catalysts as compared to

Rh and Pt-Rh catalysts. It was found that the rates of hydrogen adsorption and desorption on Pt-Rh catalyst were similar to those on Rh catalyst and much higher as compared to Pt catalyst.

The Ru-Ag bimetallic system is much simpler to study than the Pt-Rh system and serves as a model system to characterize more complicated systems such as the K/Ru system. Ag was found to decrease the amounts of adsorbed hydrogen and the hydrogen-to-ruthenium stoichiometry. Ag reduced the populations of states with low and intermediate binding energies of hydrogen on silica supported Ru catalyst. The rates of hydrogen adsorption and desorption were also lower on silica supported Ru-Ag catalyst as compared to Ru catalyst. Thus Ag influenced the kinetics and thermodynamics of hydrogen chemisorption on Ru particles and it was found that electronic and ensemble effects were not responsible for this influence of Ag. Instead, the effect of silver was due to the selective segregation of silver to the edge, corner and other defect-like sites which are proposed to be highly active for dissociative hydrogen adsorption. Hence hydrogen adsorption on Ru particles was found to be structure sensitive.

CHAPTER 1. GENERAL INTRODUCTION

Supported bimetallic catalysts are commonly used for commercial chemical reactions because these catalysts usually have higher activity, selectivity or stability as compared to monometallic catalysts (1–3). The modification of catalyst properties is most commonly explained via electronic (ligand) effects or geometric (ensemble) effects. In the case of electronic effects in bimetallic catalysts, one metal in the neighborhood of active atoms of the other metal may modify its electronic properties via electron removal/donation and thereby change its interaction with adsorbing species. Structural or geometric effects are important only for structure-sensitive reactions such as ethane hydrogenolysis which require a large ensemble of active metal atoms. Addition of a second metal may reduce the size of such an active ensemble and thus reducing the activity for that reaction. On the other hand, the second metal may form active ensembles of its own or may give rise to mixed ensembles.

A bimetallic catalyst is well characterized when we know whether bimetallic particles (or clusters) are actually formed and if they are formed, what is the surface composition of the bimetallic particles. It is also important to know whether the surface composition is uniform over all the clusters. The extent and uniformity of co-clustering in bimetallic catalysts depends on various factors such as the method of catalyst preparation and activation, type of

support, physical properties of the support, the nature of the catalyst precursors used as well as the nature and loadings of the metals in the catalyst (4).

Quantitative measurement of surface compositions is an important area of catalytic research which has not received the deserved attention. The surface compositions of bimetallic catalysts in the form of single crystals have been studied extensively (5-11) by using Auger electron spectroscopy (AES) and ion scattering spectroscopy (ISS). There are however, very few techniques available to determine the surface composition of supported bimetallic catalysts. One of the techniques is selective chemisorption. The problem is quite straightforward when Group VIII metals are combined with Group IB metals to form bimetallic clusters such as Ru-Ag or Ru-Au because it can be assumed that hydrogen does not adsorb on the Group IB metal. Supported bimetallic clusters formed between Group VIII metals such as Pt-Rh system studied here, represent a greater challenge because both metals usually adsorb most of the commonly used adsorbates such as hydrogen, carbon monoxide and oxygen. Miura et al. (12-15) have succeeded in measuring the surface compositions of a series of alumina and silica supported Pt-Ru bimetallic clusters using a selective titration technique. In this method, advantage was taken of the fact that the titration stoichiometry of the reaction between chemisorbed O_2 and gas phase CO is very different on Ru and Pt. However, it must be kept in mind while using such a technique that coadsorption of two species may result in surface reconstruction

as well as in chemisorption induced surface segregation. Adsorbates are known to influence the surface compositions of bimetallic catalysts and the effect of one adsorbate on the surface composition of the bimetallic catalyst may or may not be reversible. Wang and Schmidt (16) observed that the surface of silica supported Pt-Rh catalysts was enriched in Rh by oxidation-reduction cycling. Miura and Gonzalez (14) have used IR spectroscopic method to determine the surface compositions of Pt-Ru/SiO_2 catalysts. Wu et al. (17) used ^{1}H NMR spectroscopy to determine the surface composition of supported bimetallic catalysts. Wang et al.(18) have used ^{13}C NMR of adsorbed CO and ^{195}Pt NMR spectroscopy in order to characterize alumina supported Pt-Rh catalysts and found that the surfaces of their bimetallic catalysts were enriched in rhodium. Under reaction conditions, the surfaces of catalysts are covered with reactants and hence understanding the influence of various reactants on the surface composition of the bimetallic catalysts is important. The surface compositions of the alumina and silica supported Pt-Rh catalysts were determined in the presence of hydrogen by ^{1}H NMR which is described in Chapters 3 and 5, and in the absence of any adsorbate by ^{129}Xe NMR which is discussed in Appendix B.

Several hydrogenation reactions are carried out industrially on supported transition metal catalysts for treatment of petroleum feedstock. Further many hydrogenolysis reactions are used to gain fundamental understanding of catalytic surfaces. The mobility of hydrogen on catalytic surfaces may be

important in understanding the mechanisms of these reactions on such surfaces. as it dictates the coverage and availability of adsorbed hydrogen on the catalyst surface. Engelke et al. (19) found out that the interparticle motion of hydrogen on the surfaces of Ru/SiO_2 catalysts occurred via the gas phase and involved hydrogen adsorption-desorption processes. Hence understanding the various factors related to mobility of hydrogen and kinetics of adsorption-desorption on the surfaces of such supported catalysts is also important. The parameters related to the kinetics of adsorption and desorption processes are estimated by studying hydrogen mobility on the surfaces of these catalysts. A detailed study was done of the kinetic parameters for adsorption and desorption of hydrogen on silica supported Pt, Rh and Pt-Rh bimetallic catalysts and is described in Chapters 4 and 5. The differences in hydrogen mobility on Pt and Rh catalysts could explain the different activity exhibited by these two catalysts towards various reactions such as hydrogenolysis and isomerization.

As mentioned earlier, bimetallic catalysts consisting of Group VIII–Group IB metals are easier to characterize because hydrogen does not usually adsorb on Group IB metals and the total hydrogen uptake can be related to the fraction of Group VIII metal at the surface. The ruthenium-silver bimetallic system serves as a model system in understanding the catalytic behavior of more complicated systems involving ruthenium. The technique of ^1H NMR spectroscopy is quite suitable for this purpose because it is a quantitative technique and since silver

does not dissociatively adsorb hydrogen, the fraction of Ru atoms exposed at the surface can be directly and quantitatively determined. Further the electronic and geometric effects of Ag on Ru can also be studied by ^1H NMR with the help of atomistic simulations (20). Since there is no added complication of hydrogen spillover (21) from Ru to Ag, the study of hydrogen mobility on these surfaces can also illustrate the effect of Ag addition on catalytic properties of Ru. Hence Ru-Ag/SiO_2 catalysts were studied by ^1H NMR spectroscopy with an emphasis on the chemisorption and mobility characteristics of hydrogen on these surfaces and is described in Chapter 6. The modification of the properties of Ru by adding inactive group IB metals such as Ag may be complimentary to the modification of Ru surface by alkali metals such as potassium which is a more complicated system. It is known that potassium partitions itself between Ru metal particles and silica support (22). Thus potassium affects the chemisorption and mobility of hydrogen on the metal as well as the support. The promotional effects of potassium on Ru can be understood by studying the kinetics and energetics of hydrogen adsorption-desorption on such catalysts and based on the understanding of the simpler Ru-Ag bimetallic system. This is discussed in a separate paper in Appendix A.

Dissertation Organization

The dissertation consists of four papers (Chapters 3-6) followed by general conclusions. Each paper was written by the author in a form suitable for publication in a technical journal. The paper corresponding to Chapter 3 has been accepted in the Journal of Catalysis. The papers in Chapters 4, 5 and 6 will be submitted for publication with the author of this dissertation as the primary author. Chapters 3, 4 and 5 describe the original work carried out by the author. Chapter 6 also describes the original work done by the author along with the work on microcalorimetry done by R. L. Narayan. Appendix A describes the work done on potassium promoted Ru catalysts using ^{1}H NMR and microcalorimetry. Appendix B details the work done on Pt-Rh/Al_2O_3 catalysts by ^{129}Xe NMR spectroscopy. Appendix C describes the experimental estimation of gas phase hydrogen and compares it with calculations based on ideal gas law. Appendix D discusses the possible nature of adsorbed hydrogen labeled as α and β hydrogen along with some relevant calculations. Appendix E describes the work on interaction of CO and H_2 on Ru/SiO_2 catalyst. References for the General Introduction, Literature Review and General Conclusions chapters are given at the end of the thesis, after Appendix E.

CHAPTER 2. LITERATURE REVIEW

Theory of surface segregation

The term surface segregation refers to the enrichment of one or more components of a mixture near the surface region, relative to the bulk. Chemical models of surface segregation are of two types: Macroscopic and Microscopic models. From macroscopic thermodynamic models, only a macroscopic picture of the surface, such as the average composition for a structurally uniform surface can be obtained whereas detailed, site-specific surface composition profile can be obtained from microscopic models. The macroscopic models require the input of macroscopic thermodynamic properties such as pure component surface tensions while microscopic models require detailed bond energy information. The macroscopic models are applicable to continuum surface only whereas the microscopic models can be applied to any surface.

Gibbs (23) showed that at equilibrium, the surface excess Γ_A, of component A in a binary alloy AB is given by,

$$\Gamma_A = -(d\sigma / d\mu_A) = (N_A^{Tot} - N_A^{\alpha} + N_A^{\beta})/S \quad .....[1]$$

where μ_A is the chemical potential of component A and σ is the surface free energy of the alloy. Further, S is the interfacial area, N_A^{Tot} is the total number of moles of A in the system and N_A^{α} and N_A^{β} represent the number of moles of A in phase a

and b. (For a surface interfacing with vacuum, $N_A^{\beta} = 0$). This expression indicates that if increased amount of component A in a binary alloy AB lowers the surface free energy of the alloy then surface segregation of A would occur. However, equation [1] can not be readily used to calculate surface compositions, given only overall compositions, temperature and pressure. Hence attempts were made to develop models of predicting surface segregation, that use easily measurable or obtainable data. One such model was developed by Butler and Schuchowitzky (24,25) based on the assumptions of monolayer surface region, ideal solution behavior and equal molar surface areas of constituents. This expression, which can be used to calculate the surface compositions in terms of measurable quantities, is as follows:

$$X^S_A / X^S_B = (X^b_A / X^b_B) \exp [S(\sigma_B - \sigma_A)/RT] \quad .....[2]$$

where X^S_A and X^S_B are the first layer (surface) mole fractions of A and B, X^b_A and X^b_B are the bulk fractions of A and B, σ_A and σ_B represent the pure component surface tension for A and B, S is the surface area and T is temperature in K. The effects of the surface tension of the components and of the temperature on the surface composition of the binary system can be easily seen from equation [2]. It predicts that the component with lower surface tension will be enriched at the surface and as the temperature is increased, the surface composition approaches the bulk composition. However, the ideal solution model assumes the heat of mixing of components of a binary alloy to be zero. Other models were developed

by Guggenheim (26) and later refined by Defay and Prigogine (27), based on regular solution theory which takes into account the effects of heat of mixing.

In the microscopic models, it is suggested that the energy of the system can be described by analyzing the bonds between the metal atoms. Since bonds between atoms in the bulk have to be broken in the creation of a surface, these models are sometimes referred to as broken bond models (4). Since it is energetically favorable to break the weakest bonds, it was predicted that the component of a binary alloy having the lower heat of sublimation (bulk cohesive energy), a measure of the bulk bond strength, should segregate to the surface. However, these earlier broken bond models were not accurate because they assumed bond energies to be invariant with coordination. Another less rigorous model is the elastic strain model (4) which proposes that significant elastic strain exists in the lattice when a solute atom is placed in a matrix of atoms of unlike size. If the solute is moved to the surface, the elastic strain energy is reduced. According to this model then, the solute would segregate to the surface of an alloy whenever it is either significantly smaller or larger than the matrix atom.

The input required for the microscopic models is usually detailed information on bond energies and a symmetric mixing model. With these models, it is possible to model flat as well as structured or stepped surfaces. We can obtain microscopic information such as surface composition at basal planes, defect sites (edges and corners) and distribution of ensemble sizes, from these models.

For Pt-Rh system, the bulk cohesive energy for Rh is 554 kJ/mole which is lower than that for Pt which is 563 kJ/mole. Thus based on bulk properties, Rh segregation to the surface would be predicted. The atomic radii of Pt and Rh are 1.39 and 1.34 Å, respectively and the surface segregation behavior of this system can not be predicted based on the elastic strain model. However, these models are not accurate because these do not take into account the surface energies of Pt and Rh which would dictate the surface segregation behavior of the system. The surface energy for (111) plane is 100 kJ/mole for Pt and 110 kJ/mole for Rh in case of 31% dispersed cluster. Hence based on surface energies, platinum segregation to the surface would be predicted which is found to be correct according to many theoretical and experimental studies (5-11).

Pt-Rh bimetallic system

Adsorbate-Free Pt-Rh Surfaces

The calculations done by van Delft et al. (3) using a Monte Carlo method predict that the surface composition is almost equal to the bulk composition. Schoeb et al. (28), based on atomistic simulations for adsorbate free Pt-Rh clusters, predicted surface enrichment of Pt at 973 K.

Beck et al. (9) studied $Pt_{10}Rh_{90}$(111) crystal face in vacuum ($5x10^{-10}$ Torr) using ion scattering spectroscopy (ISS) and Auger electron spectroscopy (AES). They observed that the surface composition remained the same as the bulk composition up to 600°C, but the surface became enriched in Pt above 600°C.

Williams and Nelson (5) using ISS, observed that the surface composition was almost equal to the bulk composition at room temperature and surface was enriched with Pt at T > 800 K for disks of unsupported Pt-Rh catalysts. Similarly Pt enrichment of the (111) surface of $Pt_{0.1}Rh_{0.9}$ alloy was observed by Holloway and Williams (6) using AES at 1000 K and also by van Delft et al. (3) for (100) and (410) surfaces of $Pt_{0.25}$-$Rh_{0.75}$ alloy using AES. van Delft et al. (3) observed that Pt surface segregation increased with increasing equilibration temperature. van Langeveld and Niemantsverdriet (7) using AES observed Pt enrichment of the surface of a polycrystalline Pt-Rh alloy.

Impurity atoms may also influence the surface compositions of bimetallic catalysts. Ahmad and Tsong (29) using atom probe field ion microscopy (APFIM) found that the surface composition of Pt-Rh alloys was oscillatory in nature since the top layer of (001) plane of Pt-Rh alloys showed a significant enrichment of Rh and a considerable depletion of Rh in the second layer. The adsorbed sulfur was speculated to be the cause Rh to be enriched in surface.

Adsorbate covered surfaces

Oxygen and NO

The surface of Pt-Rh single crystals studied using AES, was found to be enriched in rhodium under the influence of oxygen, by Wolf et al. (30) and van Delft et al. (3, 8) in the temperature range of 600 to 1000 K. Williamson et al. (11) also observed by AES, the surface enrichment in Rh of Pt-Rh foils above 773 K in

the presence of oxygen. van Delft et al.(3) observed a similar effect for adsorbed NO on Pt-Rh alloys and this was attributed to the formation of oxygen adatoms upon NO dissociation.

Beck et. al. (9, 10) have examined the surface composition of $Pt_{10}Rh_{90}$(111) single crystal using ISS and AES. They also observed that the surface was enriched in rhodium in low pressure (10^{-6} Torr, T: 800-1000^{0}C) and high pressure (38 Torr, T:500-600^{0}C) oxygen environments. The authors further reported that on annealing this Rh enriched surface in the range 950-1000^{0}C, the surface became enriched in Pt again indicating that oxidation of Rh was reversible by annealing in vacuum at high temperatures. Similarly, a reducing environment could also result in a reversal of surface composition.

Wang and Schmidt (16) studied 50-200 Å diameter particles of Pt-Rh alloys and pure metals deposited on planar amorphous silica by transmission electron microscopy (TEM) and found that surface of silica supported Pt-Rh alloys was enriched in Rh after oxidation-reduction cycling. Kacimi and Duprez (30) have measured the surface composition of Pt-Rh catalysts supported on alumina using $^{18}O/^{16}O$ isotopic exchange. They observed that catalysts which were annealed in oxygen at 700^{0}C and 900^{0}C, had surface composition different from the bulk composition. Below a critical bulk Rh composition X*, the surfaces of the bimetallic catalysts were enriched in Pt and above X*, those were enriched in Rh. The composition X* was dependent on the annealing temperature.

Hydrogen and CO

Beck et al. (9) noted that the surface became enriched in Pt, from 31% Pt to 38% Pt under 10^{-6} Torr H_2. Under high pressure (38 Torr) of hydrogen, they observed (10) that the surface composition increased to 31% Pt, starting with initial composition of 4% Pt, but remained constant at 31% Pt when initial composition was 31% Pt. van Delft et. al. (8) also found that CO and H_2 do not exert a significant influence on surface composition of Pt-Rh alloys. They did not find any evidence for CO dissociation.

Zhu and Schmidt (31) studied silica supported Pt, Rh and Pt-Rh alloy particles by CO chemisorption using temperature programmed desorption (TPD). These workers observed that oxygen treatment completely suppressed CO chemisorption on Rh due to formation of an inactive Rh oxide and CO being incapable of reducing the oxide. However, oxygen treatment did not inhibit CO chemisorption on Pt. Alloy particles were transformed entirely to Rh_2O_3 with no exposed Pt atoms under the presence of oxygen at high temperatures. Reduction of this oxide in H_2 produced a surface whose CO chemisorption properties appear to be those of Rh. There was no evidence of CO dissociation on the surface of Pt, Rh or their alloys.

Oh and Carpenter (32) studied Pt, Rh and Pt-Rh bimetallic catalysts by measuring the activity of these catalysts for the CO oxidation reaction. They noted that Pt was more active for strongly oxidizing conditions and Rh was more

active for net reducing conditions. They also noted some synergism between Pt and Rh in the bimetallic catalyst which was explained in terms of geometric as well as electronic effects.

Wang (33) used ^{13}C NMR to characterize Pt-Rh bimetallic clusters with adsorbed CO and supported on η-Al_2O_3. The author has discussed two possible extreme situations for the electronic structure of Pt-Rh alloy surfaces: (i) Pt and Rh electronic wave functions maintained their local electronic structure. CO adsorbed on these (assumed to be linearly bonded) had different electronic structure for Pt and Rh, resulting in two peaks in NMR spectra with peak positions same as those on pure metal surfaces. Relative intensity of the peaks would change with surface composition of the bimetallic catalysts. (ii) Pt and Rh electronic wave functions were highly delocalized and collective behavior of electrons was important. So there should be single peak with same Knight shift in the spectra and the peak position would change with surface composition. The author could not resolve these two cases from ^{13}CO NMR lineshapes alone because, owing to broad lines, linewidths were comparable to the difference in line positions on Pt and Rh. He used ^{13}C-^{195}Pt SEDOR (spin echo double resonance) experiment as a technique to distinguish CO attached to Pt from that attached to Rh. The SEDOR experiment gave results which agree with the "delocalized picture". ^{13}CO NMR lineshift was found to be independent of CO coverage which

also indicated that CO did not preferentially bond to one metal than to the other, which again supported the "delocalized picture" for Pt-Rh bimetallic clusters.

Since CO may bind more strongly to Rh than Pt, the author tried to investigate whether the Rh segregation was induced by CO, by doing a ^{195}Pt NMR experiment. The essential features of ^{195}Pt NMR are two peaks; a "bulk" peak and a "surface" peak. The author (33) found that the position of the Pt line due to surface Pt atoms was the same both on clean and CO covered bimetallic surface. This indicated that the Rh enrichment of the surface was not caused by adsorbed CO. He has attributed it to the oxidation-reduction pretreatment given to their catalysts.

Thus the general observation has been that oxygen induces segregation of Rh to the surface of Pt-Rh bimetallic catalysts. The adsorbates CO and H_2 have been found to have no effect on surface composition of the bimetallic catalysts.

Ru-Ag bimetallic system

The Ru-Ag bimetallic system serves as a model system to study the chemisorption and mobility behavior of hydrogen. Strohl and King (20) using atomistic simulations found that silver segregates to the surface of Ru-Ag bimetallics. Wu et al.(34) also found by ^{1}H NMR that silver segregated to the surface of Ru-Ag/SiO_2 catalysts but to a lesser extent than copper in case of the Ru-Cu system. Based on atomistic simulations of the Ru-Ag system (20, 35), it is known that silver preferentially occupies the defect like edge and corner sites on

Ru surface and forms two dimensional islands at higher silver contents. This has been also supported by the recent experimental evidence of Schick et al.(36) based on various surface spectroscopic techniques. Based on data obtained by photoemission of adsorbed xenon (PAX) spectroscopy, they reported that silver preferentially decorated Ru step sites on a stepped Ru $(10\bar{1}17)$ surface whereas silver showed a tendency to form two dimensional islands on a flat Ru(0001) surface. This was further supported by other methods such as angle resolved ultraviolet photoemission spectroscopy (ARUPS), Auger electron spectroscopy (AES), low energy electron diffraction (LEED) and thermal desorption spectroscopy (TDS).

Wu et al.(34) noted by ^1H NMR that silver does not interact with ruthenium as strongly as copper. Based on evidence from X-ray photoemission spectroscopy (XPS) and X-ray excited Auger electron spectroscopy (XAES), Rodriguez (37) found that silver does not exhibit any electronic interaction with Ag. Smale and King (35) also ruled out such an effect for Ru-Ag/SiO_2 catalysts. However Rodriguez (37) proposed that there are changes in the valence bands of Ru and Ag which result in increase in the strength of the Ag-CO bond and weakening in the Ru-CO bond. This was attributed to a decrease in π backdonation from Ru to CO in the presence of Ag. From temperature programmed desorption (TPD) data, he also observed that Ag adatoms block the adsorption of CO and O_2 on Ru(0001) on a one-to-one basis.

Bernasek and Somorjai (38) observed that the hydrogen-deuterium exchange reaction occurred mainly at the defect like step sites and these defect like sites are thought to be highly active for the dissociative hydrogen adsorption and associative hydrogen desorption processes. Smale and King(35) observed that the Ru-Ag/SiO_2 catalysts were less active for ethane hydrogenolysis than Ru/SiO_2 catalysts, at all temperatures. The activity for the reaction decreased with increasing silver content and became more or less constant at 30 atomic % silver. Since ethane hydrogenolysis involves dehydrogenated intermediate species, hydrogen removal from the surface was important because otherwise hydrogen would act as an inhibitor for the reaction. It was proposed by Smale and King (35) that the defect like sites are active for hydrogen desorption from the surface and since silver blocked these sites, hydrogen desorption was prevented which resulted in lower activity for the reaction. Bhatia et al. (39) also used similar arguments to explain their ^1H NMR results on Ru/SiO_2 and Ru-Ag/SiO_2 catalysts. They observed two adsorbed states of hydrogen termed α and β, on the surfaces of these catalysts. They also observed that the population of a weakly bound species of hydrogen (termed as β resonance) was reduced by addition of silver. It was proposed that the beta hydrogen population depends on hydrogen adsorption and desorption at the defect like sites. Since silver suppressed these processes by blocking the edge and corner sites, it reduced the population of the beta hydrogen.

CHAPTER 7. GENERAL CONCLUSIONS

The surface compositions of alumina and silica supported Pt-Rh catalysts were found to be influenced by chemisorbed hydrogen. The surfaces of the Pt-Rh bimetallic catalysts were enriched in Rh under hydrogen atmosphere as opposed to the adsorbate-free Pt-Rh surfaces which are enriched in Pt. It was also found that Pt-Rh catalysts mainly consisted of bimetallic particles with fairly uniform compositions. Further, the heat of adsorption of hydrogen was found to be about 10 to 15 kJ/mole higher on Rh catalysts as compared to Pt catalysts. This understanding can be generalized to predict qualitatively and quantitatively, the surface segregation behavior of a bimetallic system under reaction conditions.

The mobility of hydrogen on Rh and Pt-Rh catalysts was higher than that on Pt catalyst. The rate constants for adsorption and desorption as well as the apparent sticking coefficients were found to be higher on Rh and Pt-Rh than those on Pt. The activation energy for hydrogen desorption was higher on Rh and Pt-Rh than that on Pt while the pre-exponential factors for the desorption rate constant were also higher on Rh and Pt-Rh catalysts as compared to Pt catalyst. The sticking coefficients of hydrogen were higher on supported metal catalysts as compared to single crystal metal surfaces which suggested that the defect-like sites are active for trapping and dissociative adsorption of hydrogen.

The amount of hydrogen adsorbed on Ru particles and the hydrogen-to-ruthenium stoichiometry decreased with increasing Ag content in the case of silica supported Ru-Ag bimetallic catalysts. It was also observed that the desorption and adsorption rates on Ru-Ag/SiO_2 catalyst were lower than those on Ru/SiO_2 catalyst. The populations of states with low and intermediate binding energies of hydrogen were lower on Ru-Ag catalyst as compared to Ru catalyst. This influence of Ag on the dynamics and energetics of hydrogen on Ru particles was not due to ensemble or electronic effects, but was a result of structure-sensitive hydrogen adsorption. Our results support the hypothesis that the low coordination sites are active for hydrogen chemisorption and blocking of these sites by Ag hinders the process significantly. This type of site specific surface segregation can be useful in tailor-making catalysts for reactions where selectivity towards some intermediate product is governed by the concentration of surface hydrogen and the kinetics of hydrogen adsorption-desorption.

APPENDIX B

SURFACE COMPOSITIONS OF Pt-Rh/Al_2O_3 CATALYSTS BY ^{129}Xe NMR SPECTROSCOPY

Introduction

^{129}Xe NMR spectroscopy has been widely used to study zeolites. This technique was originally introduced by Ito and Fraissard (1) who showed that ^{129}Xe NMR can be used to probe void volume, dimensions of channels and cavities, short distance crystallinity, acidity of zeolites as well as to study effects of cations, metal particles and chemisorption of gases like H_2 and CO on zeolite structure. de Menorval et al. (2) reported that this technique was useful in determining the number of metal particles inside the Pt/NaY zeolite cages. ^{129}Xe is a nucleus suitable for NMR studies because, (i) It has a nuclear spin I=1/2. (ii) It is chemically inert (non-reactive). (iii) It has high natural abundance (26.44%) (iv) It has a large, spherical electron cloud which is perturbed by physical interactions with other species or surfaces.

The chemical shift of ^{129}Xe interacting with a supported catalyst depends on various factors such as collisions between xenon atoms in the gas phase as well as the collisions with the channel walls of the support, local electric fields (when C^{2+} cations are present) and local magnetic fields (when paramagnetic species are present) [Jameson et al. (3), Ito and Fraissard (1)]. For zeolites of the type NaY_x, the chemical shift of ^{129}Xe increases linearly with xenon concentration or pressure.

At very low xenon concentration, probability of Xe-Xe collisions is very small and motion of xenon atoms is disturbed only by cage walls. So the chemical shift, δ_S = 58 ± 2 ppm obtained by extrapolating the $\delta = f[Xe]$ line to [Xe]=0, can be considered as the characteristic of the zeolite with respect to xenon interaction.

Ahn et al. (4) have characterized Pt-Cu/NaY catalysts using ^{129}Xe NMR and EXAFS (extended X-ray absorption fine structure). The authors suggested that for the Pt-Cu bimetallic catalysts, the chemical shift of xenon was given by an expression,

$$\delta = (\delta_{Pt} n_{Pt} + \delta_{Cu} n_{Cu} + \delta_{sup} n_{sup}) / n \qquad .....[1]$$

$$\text{where } n = n_{Pt} + n_{Cu} + n_{sup} \qquad .....[2]$$

where n_{Pt}, n_{Cu} and n_{sup} are the number of xenon atoms adsorbed on Pt clusters, Cu clusters and NaY zeolite, respectively and δ_{sup} is the chemical shift of adsorbed xenon on pure NaY zeolite at the same xenon pressure as used for Pt/NaY. The authors proposed that oxygen, when chemisorbed on metallic surfaces, prohibited xenon adsorption. Hence the values of n_{sup} and n_{Pt} could be obtained from a xenon adsorption isotherm obtained after and before oxygen chemisorption, respectively.

Yang et al. (5) studied Pt-Ir bimetallic catalysts supported on NaY zeolite using ^{129}Xe NMR and ethane hydrogenolysis. They observed only one NMR peak for Pt-Ir/NaY bimetallic catalysts which implied fast exchange of xenon either between closely separated monometallic clusters of Pt and Ir or on bimetallic Pt-Ir clusters. Based on the non-linear decrease in the Xe chemical shift with

increasing Ir content, the authors claimed that bimetallic Pt-Ir clusters were formed.

Very few studies have applied the ^{129}Xe NMR technique to supported metal catalysts. Boudart et al. (6) studied the progressive penetration of adsorbates such as hydrogen and oxygen into $Pt/\gamma\text{-}Al_2O_3$ catalyst with this technique. Valenca and Boudart (7) also studied the competition between diffusion and reaction (or chemisorption) within platinum catalyst pellets with adsorbed H_2 and O_2 using ^{129}Xe NMR. They observed two distinct NMR lines under certain conditions which meant that xenon encountered two different environments as the surface reaction proceeded slowly into the pellets and the adsorption front was sharp. They observed a single NMR line under certain other conditions, which was due to single environment encountered by xenon atoms and the adsorption front being "fuzzy".

Filiminova et al. (8) using ^{129}Xe NMR characterized two $Pt/\gamma\text{-}Al_2O_3$ catalysts- Pt-I catalysts prepared from a precursor (I) containing chloride ions- H_2PtCl_6 and Pt-II catalysts prepared from a precursor (II) not containing chloride ions-$[Pt(CO)_2]_n$ complex in acetone solution. Pt-II catalysts contained platinum only in the zero oxidation state- Pt^0, whereas Pt-I catalysts contained platinum in zero (Pt^0) and +2 oxidation state (Pt^{+2}). From their results, the authors deduced that the affinity of xenon towards Pt^{+2} was weaker than that towards Pt^0, possibly

due to shielding of Pt^{+2} ions by Cl^- ions. This indicated that platinum is more accessible to xenon atoms in Pt-II catalysts than in Pt-I catalysts.

Cheung (9) studied amorphous materials such as silica and alumina by ^{129}Xe NMR at 144 K. He observed narrow resonance lines even for such amorphous materials which indicated rapid motion of xenon atoms among micropores. A parabolic dependence of the chemical shift on xenon density in the low xenon loading regime for silica, alumina and their mixtures was explained in terms of a distribution of micropore sizes.

From the literature review it can be seen that it is possible to study the surfaces of supported catalysts using ^{129}Xe NMR spectroscopy. Since xenon undergoes only weak, physical interactions with supported catalysts, the surfaces of bimetallic catalysts will not be altered in the presence of xenon. Hence our objective was to determine the surface compositions of adsorbate-free Pt-Rh/Al_2O_3 catalysts by this method.

Methods

(a) Catalyst Preparation

One platinum and one rhodium catalyst, each with a metal loading of 3 wt% and supported on γ-alumina (Johnson Matthey, BET surface area=100 m^2/g) were prepared by incipient wetness impregnation method using $H_2PtCl_6 \cdot 6H_2O$ and $Rh(NO_3)_3 \cdot 2H_2O$ (AESAR) as precursors. Appropriate amounts

of the metal salts were dissolved in deionized water and a measured amount of the alumina support was added to the solution. The resulting slurry was dried at room temperature for 20 hours and then at 393 K for 8 hours. Three Pt–Rh bimetallic catalysts with metal loadings of 3% Pt –1% Rh, 3% Pt – 3% Rh and 1% Pt – 3% Rh were prepared in a similar manner via co-impregnation. All of the catalysts were reduced in flowing hydrogen at 673 K and subsequently washed with hot deionized water to remove residual chloride. Selective hydrogen chemisorption was used to measure the dispersion of the monometallic as well as the bimetallic catalysts.

(b) Preparation of NMR samples

The NMR tubes of 10 mm O.D. were filled with about 1.4 g of catalyst sample and attached to the sample ports of an adsorption apparatus described elsewhere. Subsequently, 760 Torr of helium was introduced into the manifold and the samples were heated to 393 K for 15 min., then evacuated and dosed with 760 Torr of hydrogen. The samples were then reduced at 673 K for 2 hours introducing fresh hydrogen every 30 min. Then the samples were evacuated at 573 K overnight and cooled to room temperature. Each sample was dosed with about 600 Torr of xenon gas and was allowed to equilibrate for about 1 hr. Finally the samples were immersed in a liquid nitrogen bath to ensure that all the xenon condensed in the sample tube. The samples were sealed with an oxy-acetylene microtorch maintaining them in the liquid nitrogen bath and then weighed. The

net weight of the catalyst sample was obtained by subtracting the weight of the empty tube from the final weight of the sealed sample. The NMR experiments were carried out in a home built NMR spectrometer with a proton resonance frequency of 250 MHz. The resonance frequency for ^{129}Xe nucleus was 69 MHz in this magnetic field. Typically, 7200 scans with a repetition time of 0.5 s were taken, but sometimes larger number of scans were required to improve the signal to noise ratio.

Results and Discussion

The NMR lines actually observed on all the catalysts were much broader than expected (peak width: 4 to 6 kHz) which could be due to exchange broadening as a result of fast exchange of xenon trapped in micropores and mesopores or macropores. The peak at 0 ppm (Figs. B1, B2) is due to xenon-xenon interactions in the gas phase and this is the primary reference for shifts in all ^{129}Xe NMR spectra. The NMR line on Rh/Al_2O_3 catalyst is difficult to see but it was more easily visible at higher temperatures (Fig. B2). The peak corresponding to xenon interaction with Rh particles shifted toward the upfield direction (closer to the peak due to gas phase xenon) with increasing temperature. This is most likely due to increased exchange of xenon on Rh particles with the gas phase xenon. The spectrum for alumina support with corresponding ^{129}Xe chemical shift is shown in Fig. B3. A variation in chemical shifts was observed on the Pt-Rh bimetallic

catalysts as the overall composition changed from 0% Rh (pure Pt) to 100% Rh (pure Rh) can be seen (Fig.B1). Since we observed single line in NMR spectra, we deduced that xenon atoms must be undergoing fast exchange over platinum, rhodium and alumina sites. This fact was utilized to calculate the surface compositions of Pt-Rh bimetallic catalysts once the chemical shifts of ^{129}Xe on pure alumina and pure Pt and pure Rh particles were known. For Pt/Al_2O_3 catalyst, the chemical shift was expressed as,

$$\delta_{Pt/Al_2O_3} = \delta_{Pt} \cdot X'_{Pt} + \delta_{Al_2O_3} \cdot X'_{Al_2O_3} \qquad .....[3]$$

where X'_{Pt} and $X'_{Al_2O_3}$ were the fractions of total area occupied by Pt particles and alumina support per gram of catalyst. These were calculated as follows,

$$X'_{Pt} = ((f_{w,Pt}/M_{w,Pt}) \cdot N_0 \cdot D \cdot (4\pi r^2_{Pt})/S_{BET}) \qquad .....[4]$$

$$\text{and } X'_{Al_2O_3} = 1 - X'_{Pt} \qquad .....[5]$$

where $f_{w,Pt}$ is the weight fraction, $M_{w,Pt}$ is the molecular weight and r_{Pt} is the atomic radius of platinum respectively; D is the dispersion of the catalyst, N_0 is the Avogadro's number and S_{BET} is the BET surface area of the catalyst. Thus from this expression, we calculated the chemical shift δ_{Pt} of pure platinum particles after knowing the xenon chemical shifts for pure alumina support and alumina supported platinum catalyst for the same xenon pressure. Similar expressions were written to calculate the shift δ_{Rh} of pure rhodium particles. For Pt-Rh bimetallic catalysts supported on alumina, expression analogous to [3] was written as,

$$\delta_{Pt\text{-}Rh/Al_2O_3} = \delta_{Pt} \cdot X'_{Pt} + \delta_{Rh} \cdot X'_{Rh} + \delta_{Al_2O_3} \cdot X'_{Al_2O_3} \quad .....[6]$$

The sum ($X'_{Pt} + X'_{Rh}$) was calculated from an expression similar to equation (4) and the fraction $X'_{Al_2O_3}$ was found from the relation,

$$X'_{Al_2O_3} = 1 - (X'_{Pt} + X'_{Rh}) \quad .....[7]$$

Thus the fraction X'_{Rh} was calculated from equation [6] since all the chemical shifts in that equation are known. Then the surface mole fraction of Rh, X^s_{Rh} can be computed easily as follows,

$$X^s_{Rh} = X'_{Rh} / (X'_{Pt} + X'_{Rh}) \quad .....[8]$$

The surface compositions estimated from this procedure and shown in Fig. B4 suggest that platinum segregates to the surface of Pt-Rh bimetallic catalysts which are not influenced by any adsorbate. This result is in agreement with the atomistic simulations performed at 304 K for particles with a dispersion of 31% and in the absence of any adsorbate (see Fig. B4). Segregation of Pt to the adsorbate-free surface of Pt-Rh bimetallic catalysts has been reported in many previous theoretical and experimental studies.

Conclusions

The surface compositions of alumina supported Pt-Rh catalysts were determined in the absence of adsorbates using ^{129}Xe NMR spectroscopy. The surface was found to be enriched in platinum in the absence of adsorbates. This is in agreement with previous theoretical and experimental studies. Thus ^{129}Xe

NMR appears to be a useful, non-destructive method to examine the surfaces of supported bimetallic catalysts not influenced by chemisorption induced surface segregation.

References

1. Ito, T., and Fraissard, J., J. Chem. Phys., 76, 5275 (1990).

2. de Menorval, L. C., Fraissard, J., and Ito, T., J. Chem. Soc. Faraday Trans. I, 78, 403 (1982).

3. Jameson, A. K., Jameson, C. J., and Gutowski, H. S., J. Chem. Phys., 59, 4540 (1973).

4. Ahn, D. H., Lee, J. S., Nomura, M., Sachtler, W. M. H., Moretti, G., Woo, S. I., and Ryoo, R., J. Catal., 133, 191 (1992).

5. Yang, O. B., Woo, S. I., and Ryoo, R., J. Catal., 137, 357 (1992).

6. Boudart, M., de Menorval, L. C., Fraissard, J., and Valenca, G. P., J. Phys. Chem., 92, 4033 (1988).

7. Valenca, G. P., and Boudart, M., J. Catal., 128, 447 (1991).

8. Filiminova, S. V., Mastikhin, V. M., Smolikov, M. D., Belyi, S. S., and Duplyakin, V. K., React. Kinet. Catal. Lett., 48(1), 209 (1992).

9. Cheung, T. T. P., J. Phys. Chem., 93, 7549 (1989).

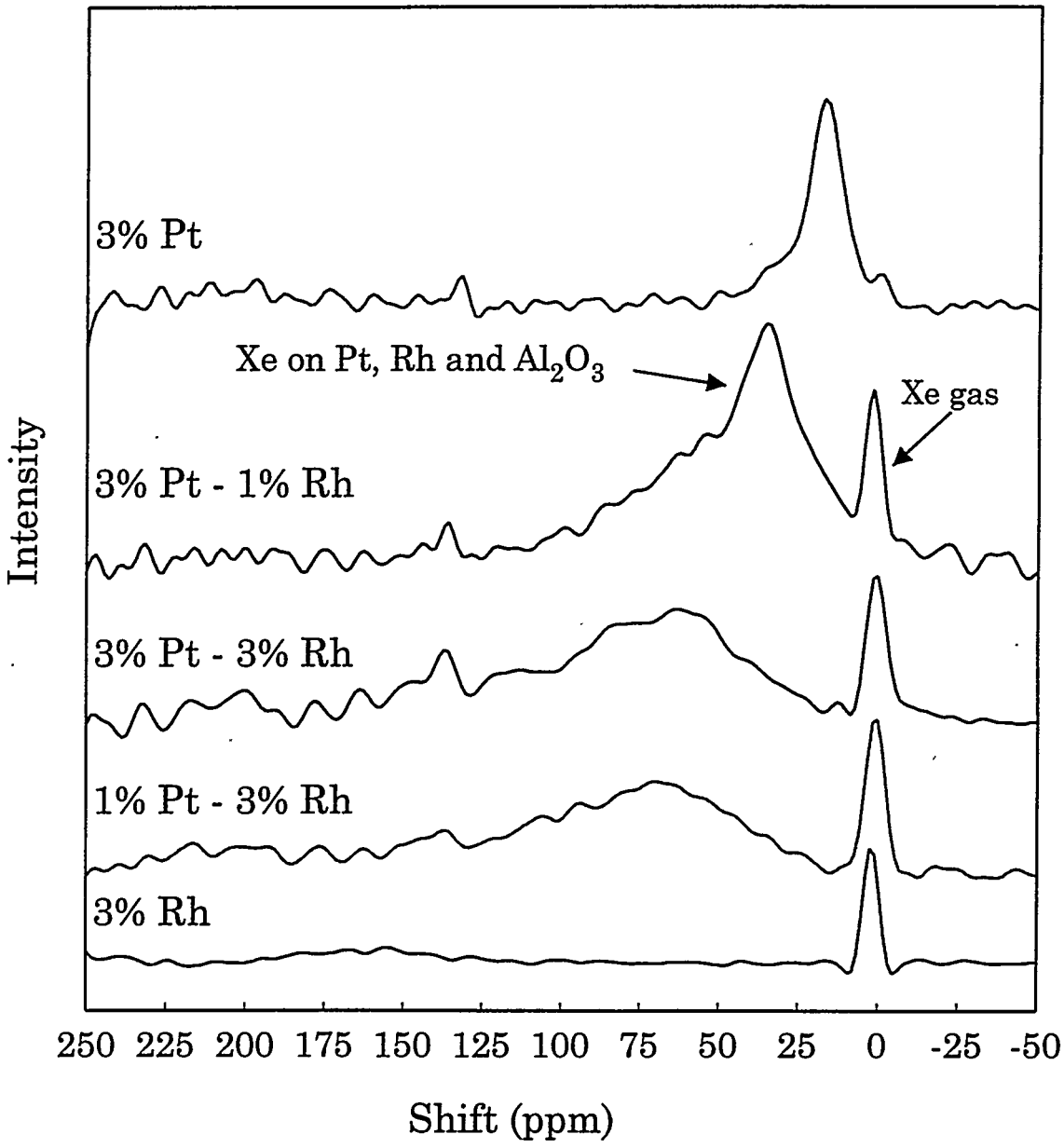

Figure B1. ^{129}Xe NMR Spectra at 600 Torr Xe for alumina supported Pt, Rh and Pt-Rh catalysts

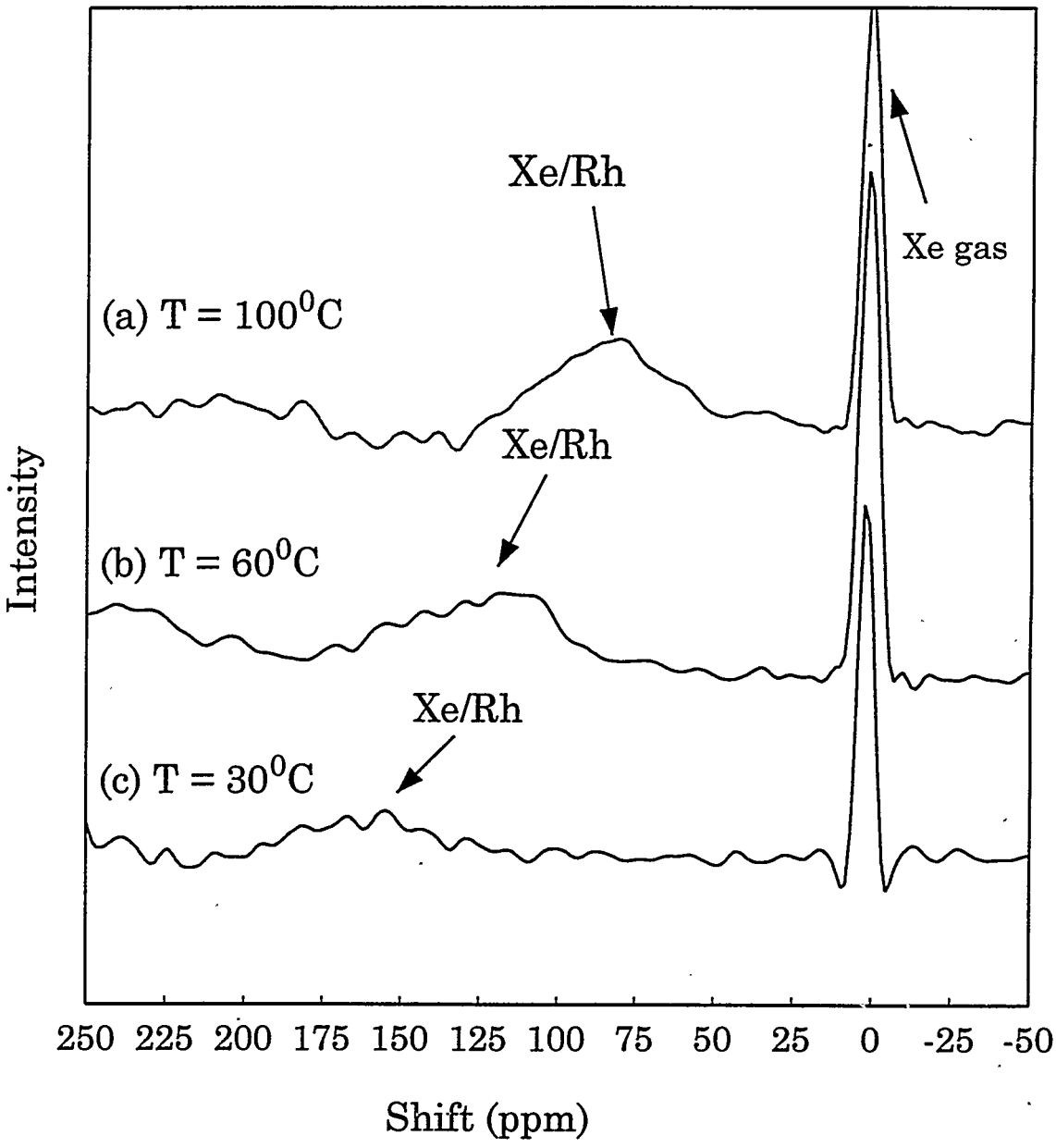

Figure B2. ^{129}Xe NMR Spectra for 3% Rh/Al_2O_3 catalyst with 600 Torr Xenon at various temperatures.

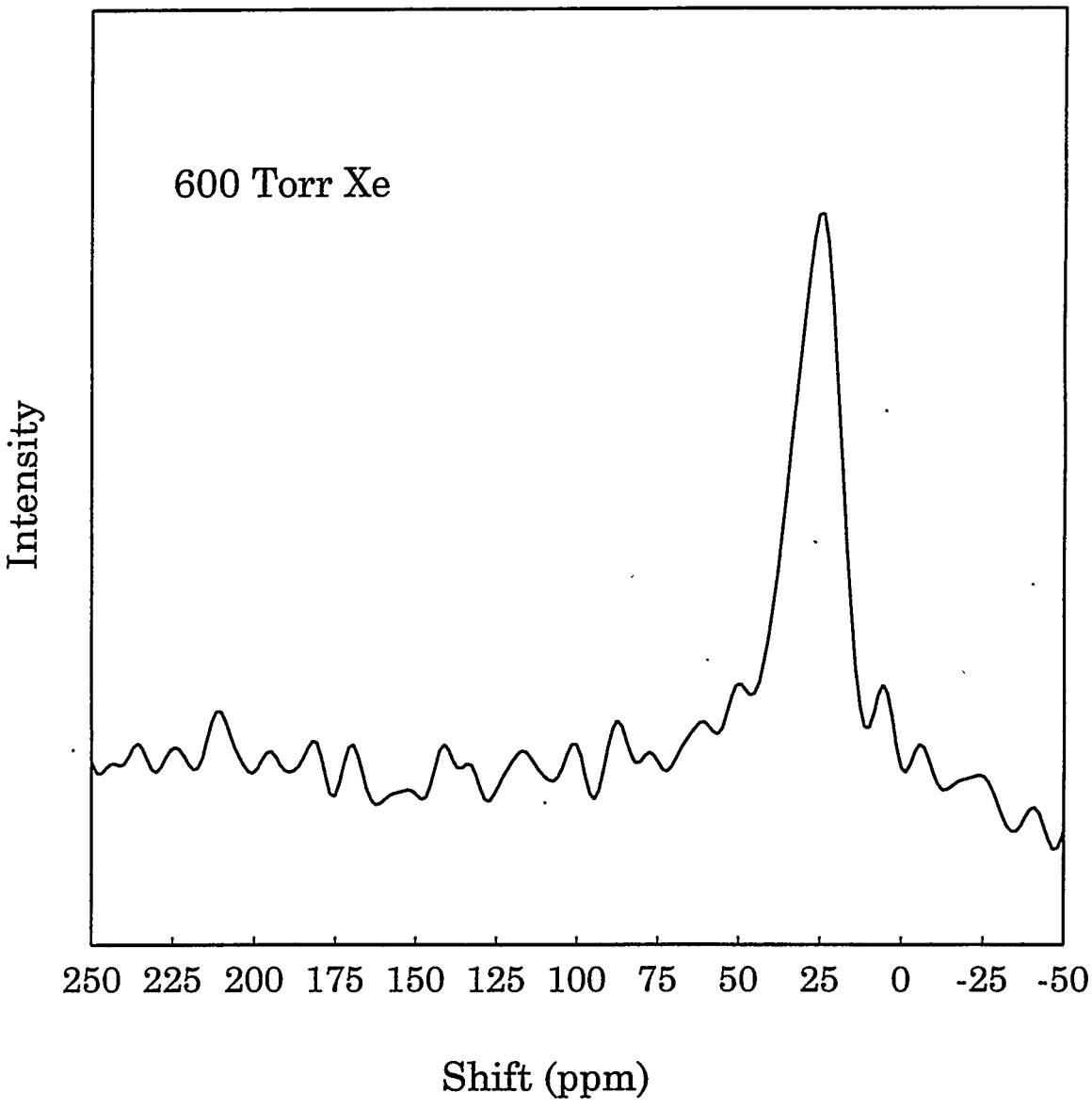

Figure B3. ^{129}Xe NMR spectrum for Al_2O_3 support

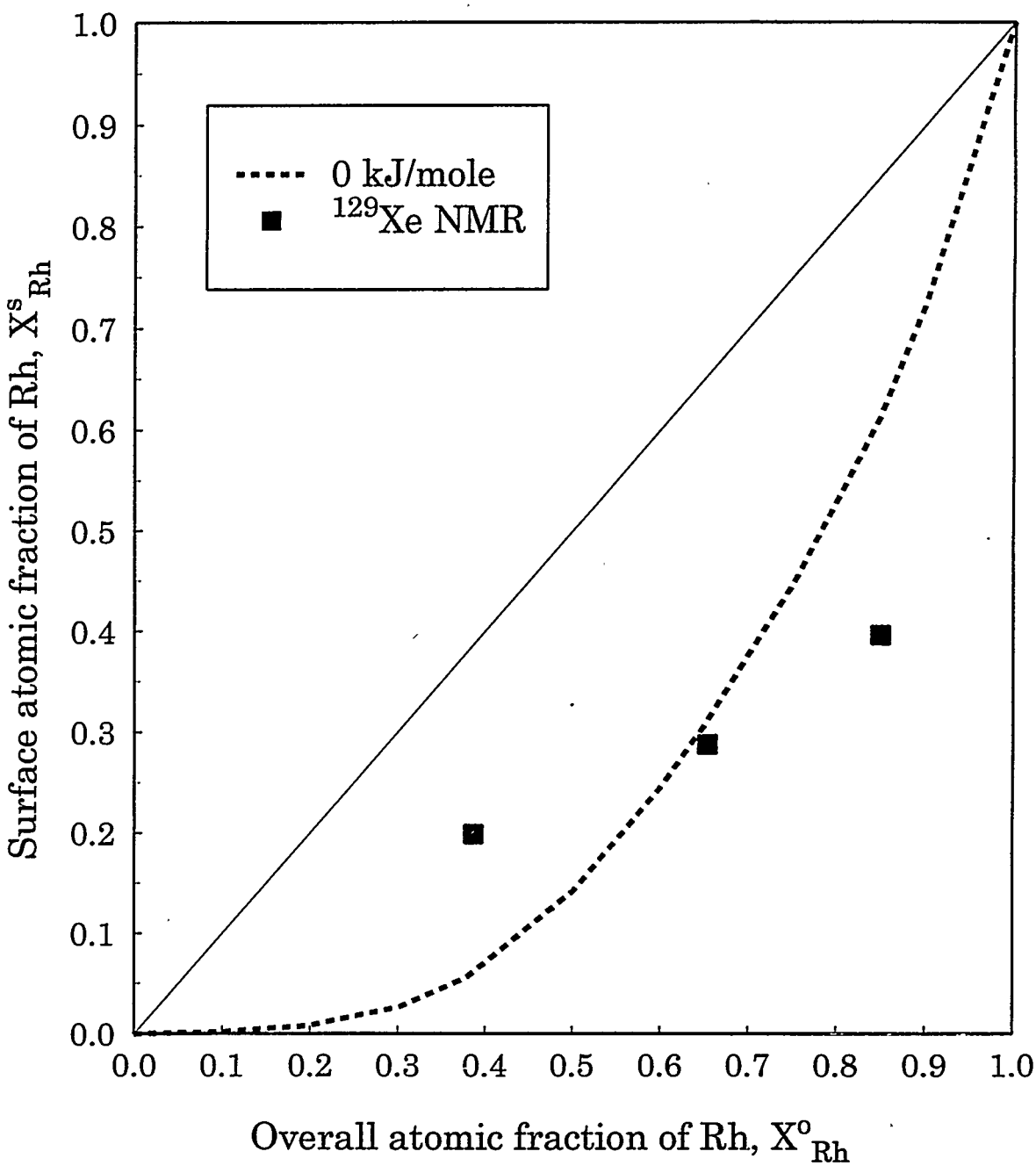

Figure B4. Surface compositions of Pt-Rh/Al_2O_3 catalysts in the absence of adsorbates

APPENDIX C

ESTIMATION OF GAS PHASE HYDROGEN

The ^1H NMR spectra of silica or alumina supported transition metal catalysts show at least two distinct resonances. The downfield diamagnetic resonance arises due to the hydroxyl groups of the support as well as hydrogen spilled over from metal particles on to the support. The upfield paramagnetic resonance arises due to the hyperfine interaction of conduction electrons of the metal with the probe nuclei, that is, ^1H spins. This second resonance corresponds to hydrogen adsorbed on the metal particles. However, this does not represent hydrogen on metal surface alone but represents hydrogen in the gas phase too because it is in fast exchange with the hydrogen on metal surface, on the NMR time scale under high pressure conditions (hydrogen pressure > 100 Torr). Hence the contribution from gas phase hydrogen to this resonance needs to be separated in order to accurately quantify the hydrogen on metal surface. This is shown here with the example of a 4% Ru/SiO_2 catalyst. In this work, it was observed that when CO was adsorbed on the surface of this catalyst at room temperature, it completely displaced the hydrogen on Ru surface as the upfield H/Ru resonance was not visible after CO adsorption (Fig. C1). When large amounts of hydrogen were adsorbed on the CO covered Ru surface, a narrow peak superimposed with the downfield peak of the support, was visible. This represented the gas phase

hydrogen which could be easily quantified by deconvoluting the peaks. This is shown in Fig. C2 for two high values of hydrogen pressure. The amount of gas phase hydrogen per surface ruthenium site ($H_{gas}/Ru_{surface}$) was also calculated from ideal gas law at various pressures, assuming that hydrogen behaves as an ideal gas. These values agree quite well with those calculated experimentally as shown in Fig. C2. This calculation based on ideal gas law is illustrated below.

(a) Diameter of NMR tube, d = 0.5 cm; length L = 2.54 cm

Porosity of catalyst $\varepsilon = 0.76$, Temperature T = 400 K

Universal gas constant R = 82.06 cm^3-atm/gmole-K

Avogadro's number $N_0 = 6.024 \times 10^{23}$ molecules/gmole

Molecular weight of ruthenium M_w = 101 g/gmole

(b) Volume of NMR tube $V = (\pi/4)d^2L = 0.4987$ cm^3

Volume of gas phase hydrogen in the tube $V_g = \varepsilon V = (0.76)(0.4987) = 0.379$ cm^3

Ideal gas law; $PV_g = n_gRT$ or number of moles of hydrogen gas,

$n_g = (PV_g)/(RT) = (P/760)(0.379)/(82.06*400) = 1.519 \times 10^{-8}$ P,

where P is pressure in Torr

Number of molecules of hydrogen gas $N_g = n_g N_0 = 9.153 \times 10^{15}$ P.

At P = 100 Torr, $N_g = 9.153 \times 10^{17}$

(c) Typical weight of catalyst in NMR tube w = 0.14 g

Weight loading of Ru catalyst w_1 = 4%

Total number of Ru atoms in the NMR sample,

$N_{Ru,\ total} = w \times w_1 \times N_0/M_w = (0.14)(0.04)(6.024 \times 10^{23}) /(101)$

$N_{Ru,\ total} = 3.37 \times 10^{19}$

Catalyst dispersion D = 8.7%

Number of surface Ru atoms in the NMR sample,

$N_{Ru,\ surface} = N_{Ru,\ total} \times D = 2.93 \times 10^{18}$

Hence, number of molecules of gas phase hydrogen per surface ruthenium site,

$H_{gas}/Ru_{surface} = (N_g/N_{Ru,\ surface}) = (9.153 \times 10^{17})/(2.93 \times 10^{18})$

$H_{gas}/Ru_{surface} = 0.312$ at 100 Torr H_2 for 4% Ru/SiO_2 catalyst with 8.7% dispersion.

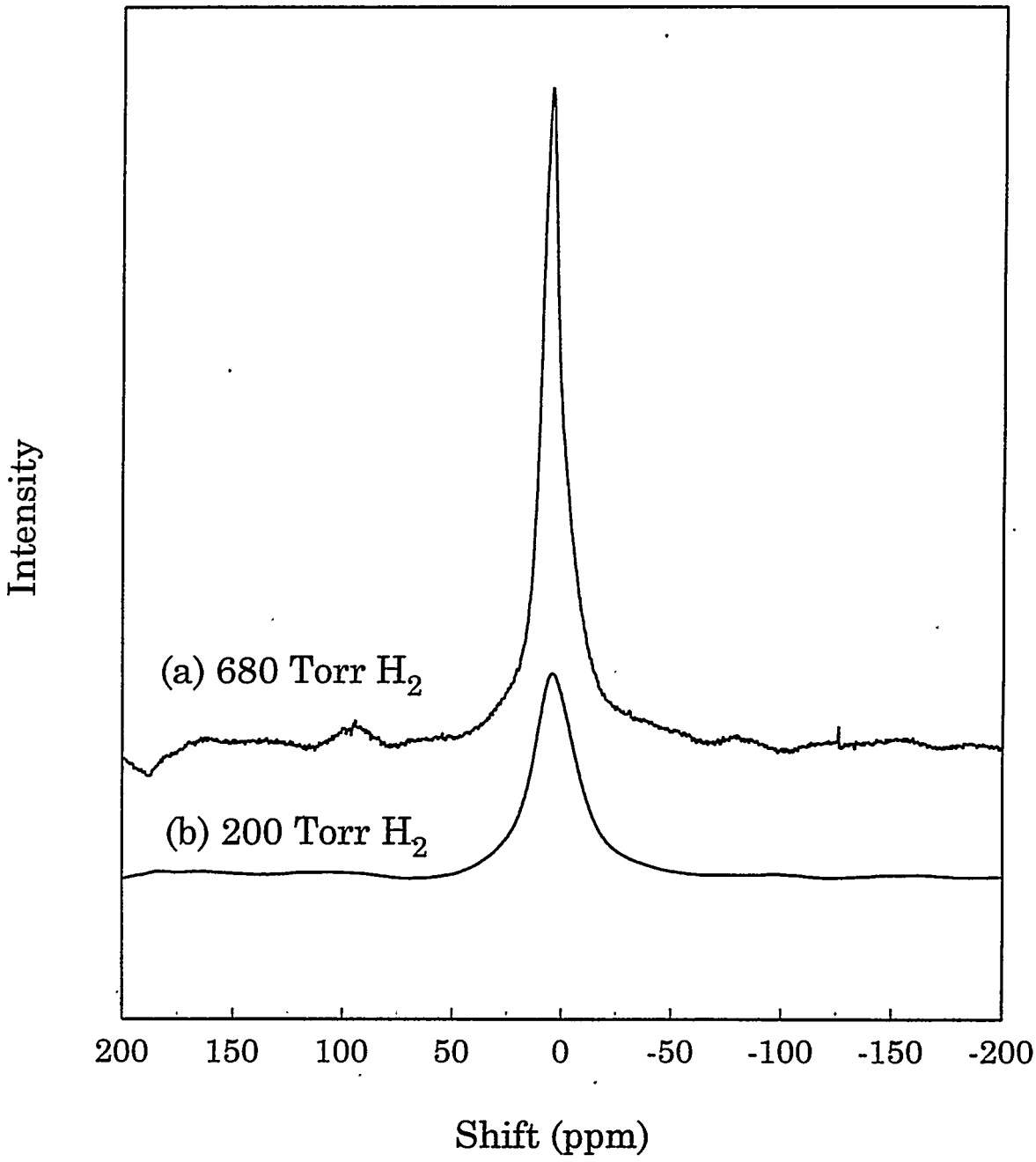

Figure C1. ^1H NMR spectra of 4% Ru/SiO_2 catalyst with (a) 680 Torr H_2 and (b) 200 Torr H_2 after saturating the surface with CO.

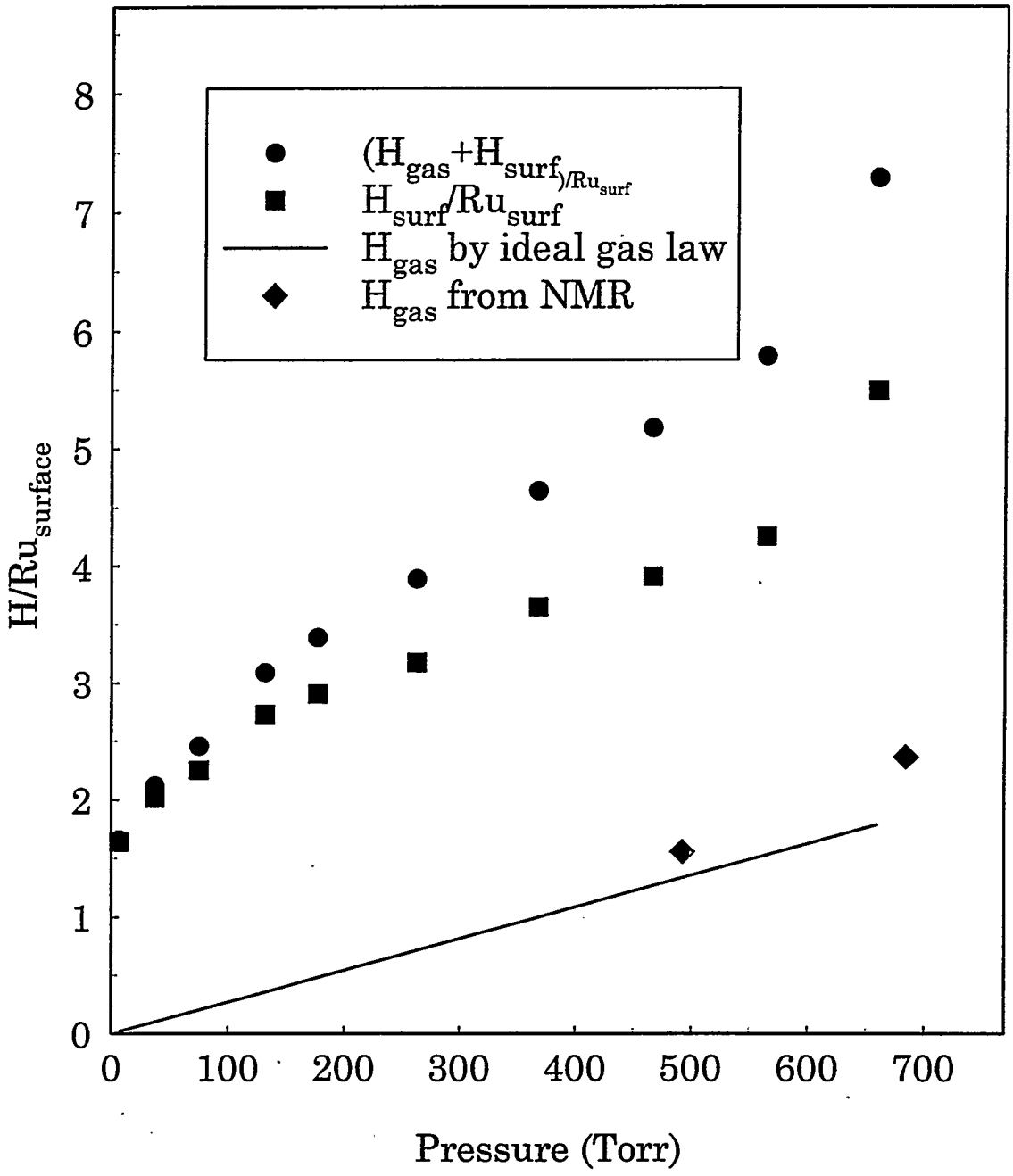

Figure C2. Estimation of gas phase hydrogen from ideal gas law (solid line) and experimentally after saturating the surface with CO (diamonds)

APPENDIX D

NATURE OF ADSORBED HYDROGEN ON Ru/SiO_2

Two peaks, termed as α and β, were observed by Bhatia et al.(1) corresponding to hydrogen adsorbed on Ru/SiO_2 catalysts. It was confirmed that the hydrogen species represented by the α peak corresponded to a strongly bound hydrogen on the surface of Ru metal particles and was speculated to occupy the three fold hollow sites. However, the exact nature and location of the hydrogen species represented by the β peak is not still clear. It is known that this peak appears only at H_2 pressures above 100 Torr and corresponds to a weakly bound species. The possible explanations for the nature and location of this species are discussed below based on some experimental results and elementary calculations.

From the data on pore size distribution, it was found that silica support has a bimodal pore distribution with mean pore diameters of 100 Å (10^{-6} cm) and 10^5Å (10^{-3} cm). The average diameter of ruthenium particles is less than 100 Å and most of these particles will reside inside such micropores. A time scale of 700 μs is used in the following calculations because Engelke et al.(2) from two dimensional ^1H NMR observed that the hydrogen corresponding to α and β peaks was in slow exchange with a time scale of 700 μs.

(a) Mean free path of hydrogen

It is given by the following expression (3):

$\lambda = [\ 1.41\pi\ \sigma^2\ n^*]^{-1}$

where σ = molecular diameter in cm and

n^* = no. of molecules per cm^2 = $[\ P\ N_0 / RT]$

$\lambda = 2.24 \times 10^{-6}\ (\ T / P\ )$

Atomic radius of H atom = 0.37 Å, hence $\sigma = 0.74 \times 10^{-8}$ cm

At T = 300 K, P = 1 atm, $\lambda = 6.64 \times 10^{-4}$ cm

P = 0.132 atm (100 Torr), $\lambda = 5.1 \times 10^{-3}$ cm

P = 0.0132 atm (10 Torr), $\lambda = 5.1 \times 10^{-2}$ cm

Depending on the pore diameter and mean free path of hydrogen at a given pressure, the diffusion of hydrogen could be either molecular type or Knudsen type. At P = 100 Torr,

For small pores, $d / \lambda = 1.95 \times 10^{-4} <<< 0.2$, hence Knudsen diffusion

For large pores, $d / \lambda = 0.196$ could be molecular diffusion or in transition region.

(b) Molecular diffusion

Diffusion coefficient of hydrogen in gas phase is given by the following empirical correlation (4):

$D_{H2} = [\ 10^{-3}\ T^{1.75}\ \{(\ M_A + M_B\ )/M_AM_B\}] / [\ P\ \{(\Sigma v_A)^{1/3} + (\Sigma v_B)^{1/3}\}]$

For H_2, $\nu_A = \nu_B = 3.96$, $M_A = M_B = 2$,

Hence $D_{H2} = 3.16 \times 10^{-4} (T^{1.75} / P)$

At T = 300 K and P = 1 atm, $D_{H2} = 6.84$ cm^2/s

(c) Knudsen diffusion

The coefficient of Knudsen diffusion is given by the following expression (5)

$D_K = (2d / 3) (8 RT / \pi M)^{1/2}$

R = 8.314×10^7 erg/gmole K, M = 2 for hydrogen

At T = 300 K, $D_K = 1.188 \times 10^5$ d

(i) For small pores, d = 10^{-6} cm, $D_K = 0.1188$ cm^2/s

$L^2 = D \tau$,

For $\tau = 700$ μs, L = 9.1×10^{-3} cm

Thus the diffusional distance traveled by hydrogen is 1000 times the average pore diameter and hence hydrogen representing α and β peaks will be in fast exchange.

(ii) For large pores, d = 10^{-3} cm, $D_K = 1.188 \times 10^2$ cm^2/s

Thus $D_K >>> D_{H2}$ and hence diffusion will be molecular..

Diffusional distance traveled by hydrogen in gas phase,

$L^2 = D \tau$ (based on Fick's law of diffusion)

For $\tau = 700$ μs, L = 0.069 cm = 6.9×10^6Å

Pore diameter for large pores is 0.001 cm and the diffusional distance traveled is 70 times the average pore diameter. Hence hydrogen representing α and β peaks will be in fast exchange with each other even within the large pores.

(d) Surface Diffusion coefficient of hydrogen

$D_S = (\lambda/4)\ (kT/2\pi m)^{1/2}$

m=1, k = 1.38×10^{-16} erg / K

At T = 300 K and P = 1 atm, $\lambda = 6.64 \times 10^{-4}$ cm

$D_S = 1.34 \times 10^{-11}$ cm^2/s

If $L^2 = D_S \tau$ then, for τ = 700 μs, L = 9.6×10^{-8} cm = 9.6 Å

If surface diffusion is the prevalent mechanism for hydrogen to diffuse then it is possible that hydrogen representing α and β peaks will be in slow exchange with each other. However, it was shown by Engelke et al.(2) that surface diffusion is not the dominant mechanism of hydrogen mobility.

Possible explanations for β state

(a) Effects of different pore sizes

The α and β states could correspond to hydrogen residing in the small and large pores respectively. It was shown above that Knudsen diffusion prevails in the smaller micropores whereas molecular hydrogen diffusion is dominant in the larger mesopores and macropores. However, diffusional distance of hydrogen is quite large over the NMR time scale for both, small and large pores, whichever

be the diffusion mechanism. Hence if hydrogen corresponding to α and β peaks represents hydrogen residing in small and large pores then there has to be fast exchange between these two species which not true. Hence these two forms of hydrogen (α and β) can not correspond to hydrogen residing in small and large pores.

(b) Surface species or spillover to support

It could be some species formed by surface diffusion since it is a slow process and could explain the lack of fast exchange between α and β states. However if it is a species which spills over to the support, the following questions are still unanswered. Why does it show large Knight shifts? and How is it different from spilled over hydrogen observed close to hydroxyl group resonance?

(c) Precursor state

β state could be a molecular precursor to α state as it can be a weakly bound species. The dissociation process could be intrinsically slow thus explaining the slow exchange between the two species. A precursor state can exist over an occupied site {Xu and Koel (6)}. If there is any correlation between appearance of β state and higher mobility of α state then it can be explained only by such precursor state. But in such a case, reduction in population should cause a reduction in α .population too. One more possibility is that β state could be just a weakly bound species which appears only at higher pressures and is independent of the existence of α state.

References

1. Bhatia, S., Engelke, F., Pruski, M., Gerstein, B. C., and King, T. S., J. Catal., 147, 455 (1994).

2. Engelke, F., Bhatia, S., King, T. S., and Pruski, M., Phys. Rev. B, 49(4), 2730 (1994).

3. Treybal, R. E., "Mass Transfer Operations", McGraw Hill, Singapore (1981),

4. Maron, S. H., and Prutton, C. F., "Principles of Physical Chemistry", Oxford and IBH Publishing Co., New Delhi (1972).

5. Smith, J. M., "Chemical Engineering Kinetics", McGraw Hill, Singapore (1981).

6. Xu, C. and Koel, B. E., J. Chem. Phys., 100 (1), 664 (1994).

APPENDIX E

INTERACTION OF H_2 AND CO ON Ru/SiO_2

Introduction

Several research efforts have been concentrated on the study of Fischer-Tropsch reaction for coal liquefaction because liquid fuels are cheaper and more efficient in many ways than solid or gaseous fuels. Hydrogenation of carbon monoxide over supported metal catalysts has also been studied extensively because this is the first step in the production of liquid hydrocarbon fuels by Fischer-Tropsch synthesis. On industrial scale, iron and cobalt are used as catalysts for Fischer-Tropsch synthesis (1). For academic research, ruthenium is used because it gives much simpler products consisting of linear olefins, paraffins and relatively few oxygenated products and it does not form bulk carbide like iron and cobalt do, under reaction conditions (2).

Originally Fischer and Tropsch (3) assumed metal carbides to be the reaction intermediates. This was contradicted by Kummer et al.(4) who proposed that oxygen containing surface complexes such as CHO(ads) or HCHO(ads) were reaction intermediates and this was supported by the work of Dalla Betta et al.(5) and Vannice (6) on Ru catalysts. However, more recent studies by Ekerdt and Bell (7) and Biloen et al.(8) on Ru catalysts have supported the hypothesis that surface carbon atoms, generated by dissociation of

CO are the actual reaction intermediates. This surface carbon is hydrogenated to produce adosorbed methylene and methyl groups and it is proposed that the methyl groups act as precursors for the formation of methane as well as for the growth of hydrocarbon chains. This has also been supported by the work of Brady and Petit (9) who showed that a spectrum of hydrocarbons can be formed by the reaction of CH_2N_2 and H_2 over Ru and other Group VIII metals. Ekerdt and Bell (7) also suggested that hydrogenation of surface carbon atoms can occur even after the elimination of chemisorbed CO from the surface. Although Dalla Betta and Shelef (10) have proposed that CO dissociation is the rate controlling step for CO hydrogenation, Biloen et al.(8) showed using isotopic tracer studies that CO dissociation is very rapid on Ru and unlikely to be the rate limiting process. Biloen et al. (8) proposed that the conversion of C_1 species to C_2 species was rate controlling and Kobori et al.(11) have supported this proposal by mechanistic study of CO hydrogenation over Ru/SiO_2 and Ru black.

In this study, we have examined the interaction of CO and H_2 on Ru/SiO_2 catalyst by ^1H NMR. Since NMR is a quantitative method, surface coverage of adsorbed hydrogen and hydrocarbon species can be directly measured. Based on this, the surface coverage of CO can also be deduced. The objective was to examine the kinetics of CO hydrogenation and determine the reaction orders with respect to coverage of surface species. The rate constants and activation energy was also determined from this study and compared with previous studies.

Methods

The Ru/SiO_2 catalyst was prepared according a method described elsewhere (12). The catalyst was reduced in hydrogen for 1.5 hrs at 673 K dosing fresh hydrogen every 30 min. The sample was cooled to room temperature and reaction of hydrogen with CO on Ru/SiO_2 catalysts was monitored via ^1H NMR spectroscopy. The catalyst sample was dosed with about 50 Torr CO at room temperature and allowed to equilibrate for an hour. The CO was then evacuated for 30 min. at room temperature and heating was started after stopping the evacuation. After a certain desirable temperature was reached, hydrogen was dosed at a pressure of about 460 Torr and the kinetics of the reaction was monitored via ^1H NMR spectroscopy by recording the spectra at various time intervals.

Results and Discussion

Two peaks were seen due to H/Ru on the catalyst at all times in the NMR spectra although they were not apparent in the beginning (Fig. E1). These peaks were labeled as α and β resonances (12). Quantification of the spectra yielded the values of $H/Ru_{surface}$ with time, for both α and β peaks (Fig. E2). It is known that the α resonance is associated with hydrogen adsorbed on the surface

of ruthenium particles. Hence this peak was considered as a measure of the surface coverage of CO and the CO coverage was calculated as follows:

$$[CO/Ru_{surf}] = [1- \{ (H/Ru_{surf})/(H/Ru_{surf})_{sat}\}]$$

If the reaction kinetics is such that the reaction is first order in CO surface coverage and zero order in H_2 surface coverage then we can write,

$$r = -d\theta_{CO}/dt = k\theta_{CO}$$

where k is the rate constant for the reaction and θ_{CO} is the surface coverage of CO. Upon integrating this equation, it can be seen that a plot of $\ln\{[CO]/[CO]_{initial}\}$ versus time would be a straight line with a slope equal to the rate constant k. Such a plot was indeed found to be a straight line and value of k was obtained from this plot (Fig. E3). The rate constants obtained are in the range of 10^{-3} to 10^{-4} s^{-1} which is comparable to the range of 10^{-2} to 10^{-4} s^{-1} reported by Dautzenberg et al.(13) but much smaller than the range of about 0.1 to 1 s^{-1} reported by Komaya et al.(14).

The reaction was carried out at different temperatures and the quantities mentioned above were plotted to obtain values of k as a function of temperature. An Arrhenius plot of lnk versus 1/T yielded a value of 54 kJ/mole for activation energy (Fig. E4). This value appears to be much lower than a value of about 100 kJ/mole reported for the activation energy of CO hydrogenation reaction on Ru catalysts (5-7). Further, Ekerdt and Bell (7) observed reaction order of –0.6 with respect to CO partial pressure and of 1.5 with respect to H_2 partial pressure,

consistent with the results of Vannice (6). However, we are assuming an order of 1 with respect to surface coverage of CO and an order of zero with respect to surface coverage of hydrogen. This is consistent with the hypothesis of Dalla Betta (5) et al. that CO dissociation is the rate controlling step. However, it is in contradiction to the hypothesis of Ekerdt and Bell (7) and Biloen et al.(8) who proposed that the hydrogenation of C_1 species to C_2 species is the rate limiting step.

The main products observed by Ekerdt and Bell (7) were methane, ethane, propane and propylene. However, it needs to be clarified in our case whether CO and hydrogen are actually reacting on Ru surface. Although Kobori et al.(11) report that the surface hydrocarbon species occupy only a small fraction of Ru surface as most of the surface is covered with adsorbed CO, large amounts of hydrocarbons desorbing from the surface are expected to be present in the gas phase. However, peaks corresponding to gas phase products such as methane or water are not seen in our ^1H NMR spectra. Hence formation of products needs to be investigated via other techniques such as mass spectrometry or IR spectroscopy.

The reaction may not be occurring because CO might be desorbing from the surface at higher temperatures. The following experiment was carried out to check this possibility. At room temperature, even though hydrogen was dosed on a surface saturated with CO, peaks due to H/Ru were not seen even after

waiting for long time intervals which suggested that hydrogen was not able to displace CO adsorbed on Ru surface at room temperature. This was also observed at 400 K by doing the following experiment. The CO on Ru surface was allowed to equilibrate and then evacuate at room temperature. The temperature was then raised to 400 K and maintained for 1 hour without any exposure to hydrogen. Then the sample was cooled back to room temperature and hydrogen was dosed at 460 Torr. Again H/Ru peaks could not be seen which suggested that CO did not desorb from Ru surface at 400 K.

The other possibility is that hydrogen is assisting CO desorption at higher temperatures. In that case, we are measuring the kinetics of CO desorption instead of reaction kinetics. Gland et al.(15) observed that chemisorbed CO was displaced from the surfaces of Ni(100) and Pt(111) by hydrogen in the range of 309 to 328 K. Adsorbed CO was removed about 5 times faster in the presence of hydrogen than in the absence of hydrogen which suggested that displacement of CO was occurring in the presence of hydrogen. The thermal activation energies for the displacement process were found to be in the rage of 8 to 12 kcal/mol. The displacement rates were first order in CO suggesting that single adsorbed CO molecule was involved in the rate-limiting step. Displacement of adsorbed CO by hydrogen was also observed by Zhang and Gellman (16) on Ni(111) surface in the hydrogen pressure range of 10^{-9} to 10 Torr. They reported a net decrease in the CO desorption energy from 30 kcal/mol in ultrahigh vacuum to

22 kcal/mol in the presence of hydrogen. The influence of hydrogen on the CO desorption kinetics could be due to a shift of CO molecules from linear to bridging sites in the presence of hydrogen. The initial (zero coverage) heat of adsorption of CO on Ru/C at 423 K is reported to be 138 kJ/mol according to calorimetric measurements (17) which is much higher than the value of 54 kJ/mole obtained in this work. However, the heat of adsorption is a strong function of coverage. For Pt/SiO_2 catalysts, the heat of adsorption of CO varies from 150 to 10 kJ/mole as the coverage varies from 0 to 0.4, at 390 K (17). Since the CO coverage is varying from 1 to 0 in our case, we might be observing the heat of adsorption averaged over the entire range of coverages.

Conclusions

It needs to be confirmed whether CO and H_2 are reacting on the surface of Ru/SiO_2 since peaks due to products such as gas phase methane and water are not seen in the ^1H NMR spectra. If there is a reaction occurring, it appears to be first order in CO surface coverage and zeroth order in H_2 surface coverage.

References

1. Biloen, P., and Sachtler, W. M. H., Advances in Catalysis, 30, 165 (1981)

2. Kellner, C. S., and Bell, A. T., J. Catal., 70, 418 (1981).

3. Fischer, F., and Tropsch, H., Brennst. Chem., 7, 97 (1926).

4. Kummer, J. T., De Witt, T. W., and Emett, P. H., J. Amer. Chem. Soc., 70, 3632 (1948).

5. Dalla Betta, R. A., Piken, A. G., and Shelef, M., J. Catal., 35, 54 (1974).

6. Vannice, M. A., J. Catal., 50, 228 (1977).

7. Ekerdt, J. G., and Bell, A. T., J. Catal., 58, 170 (1979).

8. Biloen, P., Helle, J. N., and Sachtler, W. M. H., J. Catal., 58, 95 (1979).

9. Brady, G. III, and Pettit, R., J. Amer. Chem. Soc., 102, 6181 (1980).

10. Dalla Betta, and Shelef, M., J. Catal., 49, 383 (1977).

11. Kobori, Y., Yamasaki, H., Naito, S., Onishi, T., and Tamaru, K., J. Chem. Soc. Faraday Trans. I, 78, 1473 (1982).

12. Bhatia, S., Engelke, F., Pruski, M., Gerstein, B. C., and King, T. S., J. Catal., 147, 455 (1994).

13. Dautzenberg, F. M., Helle, J. N., van Santen, R., A., and Verbeek, H., J. Catal., 50, 8 (1977).

14. Komaya, T., and Bell, A. T., J. Catal., 146, 237 (1994).

15. Gland, J. L., Fischer, D. A., Shen, S., and Zaera, F., J. Am. Chem. Soc., 112, 5695 (1990).

16. Zhang, R., and Gellman, A. J., Langmuir, 9(2), 449 (1993).

17. Cardona-Martinez, N., and Dumesic, J., Advances in Catalysis, 38, 149 (1992).

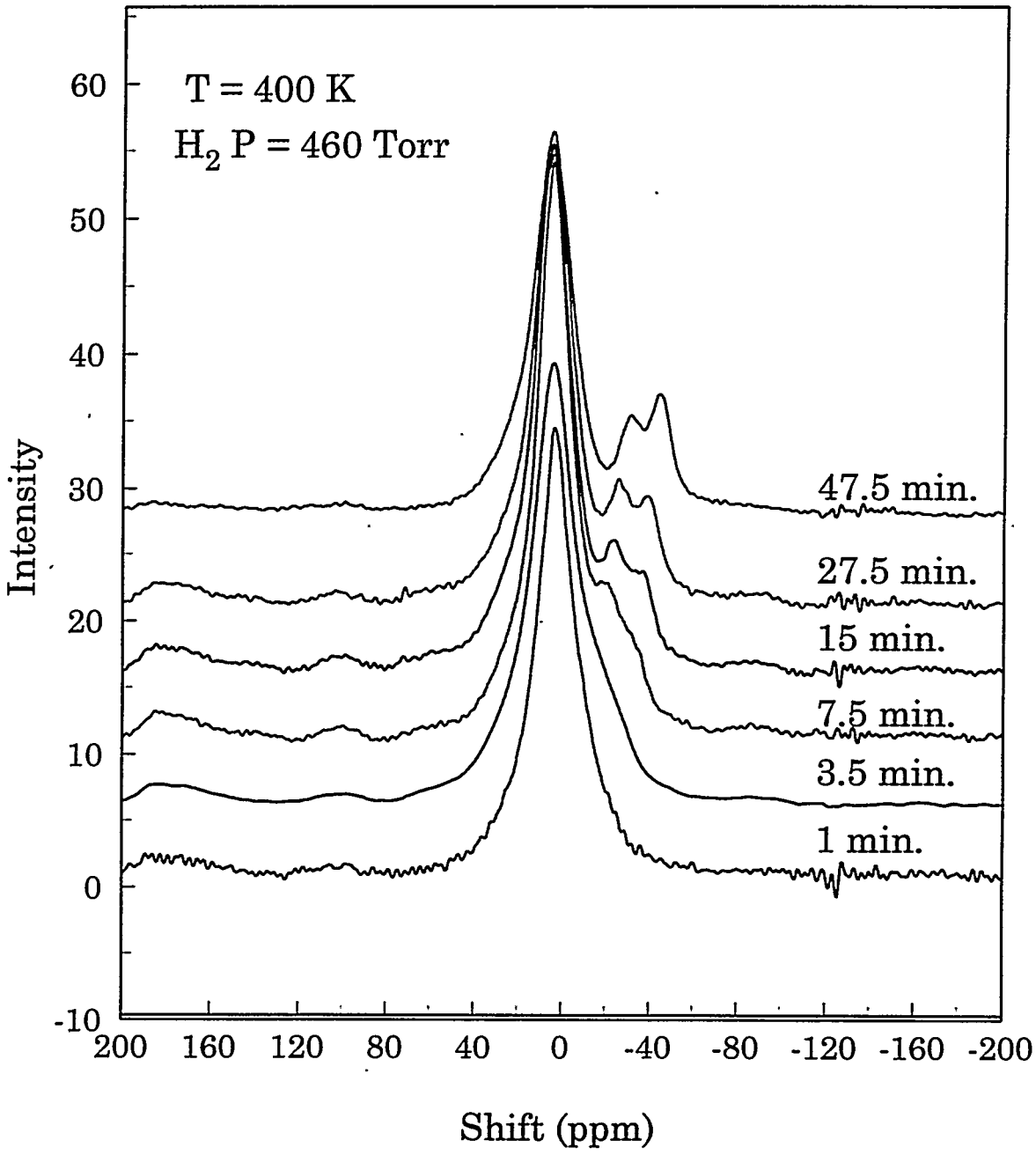

Figure E1. ^1H NMR spectra for reaction of H_2 with CO at various time intervals

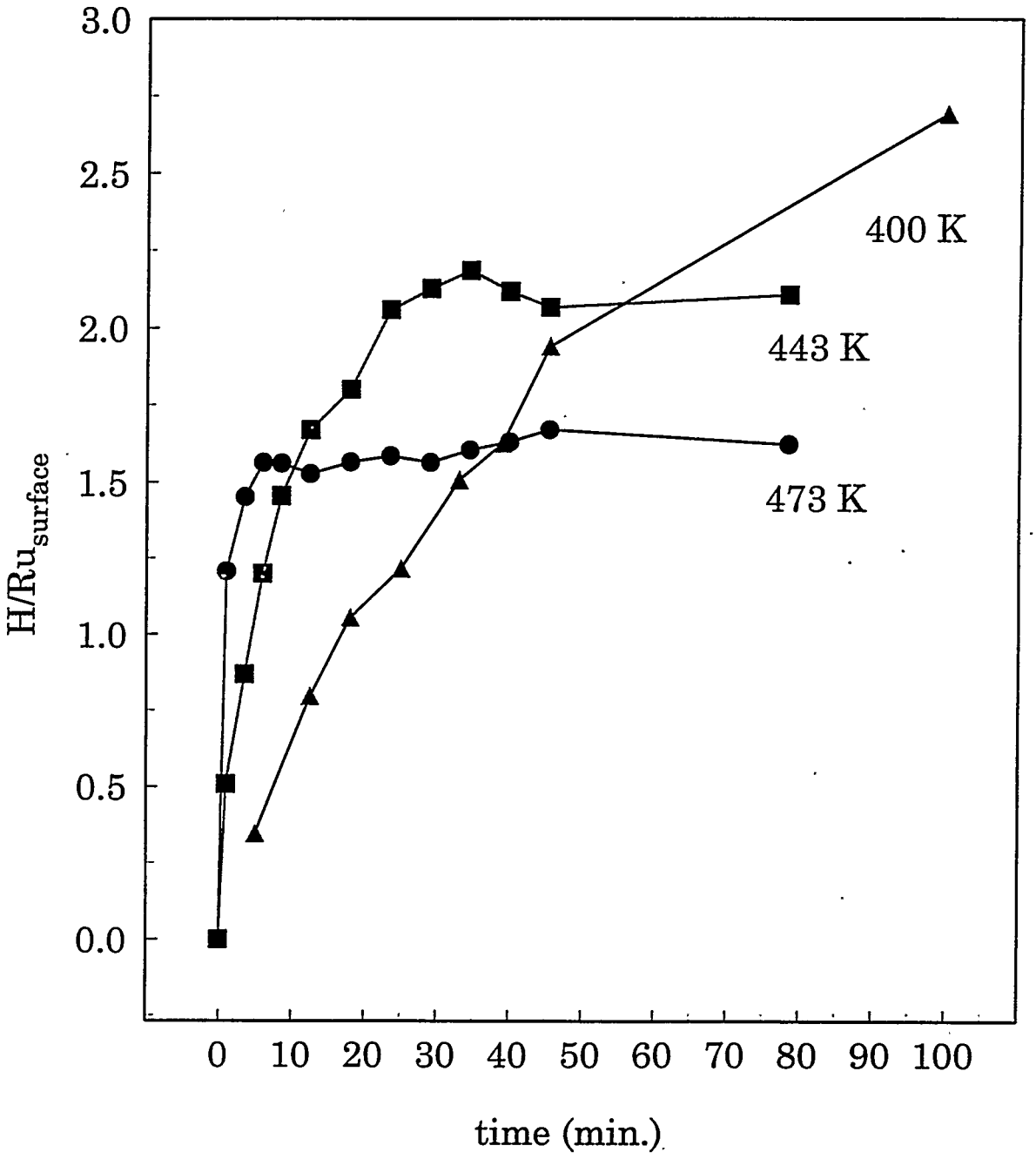

Figure E2. A logarithmic plot of normalized CO concentration with time

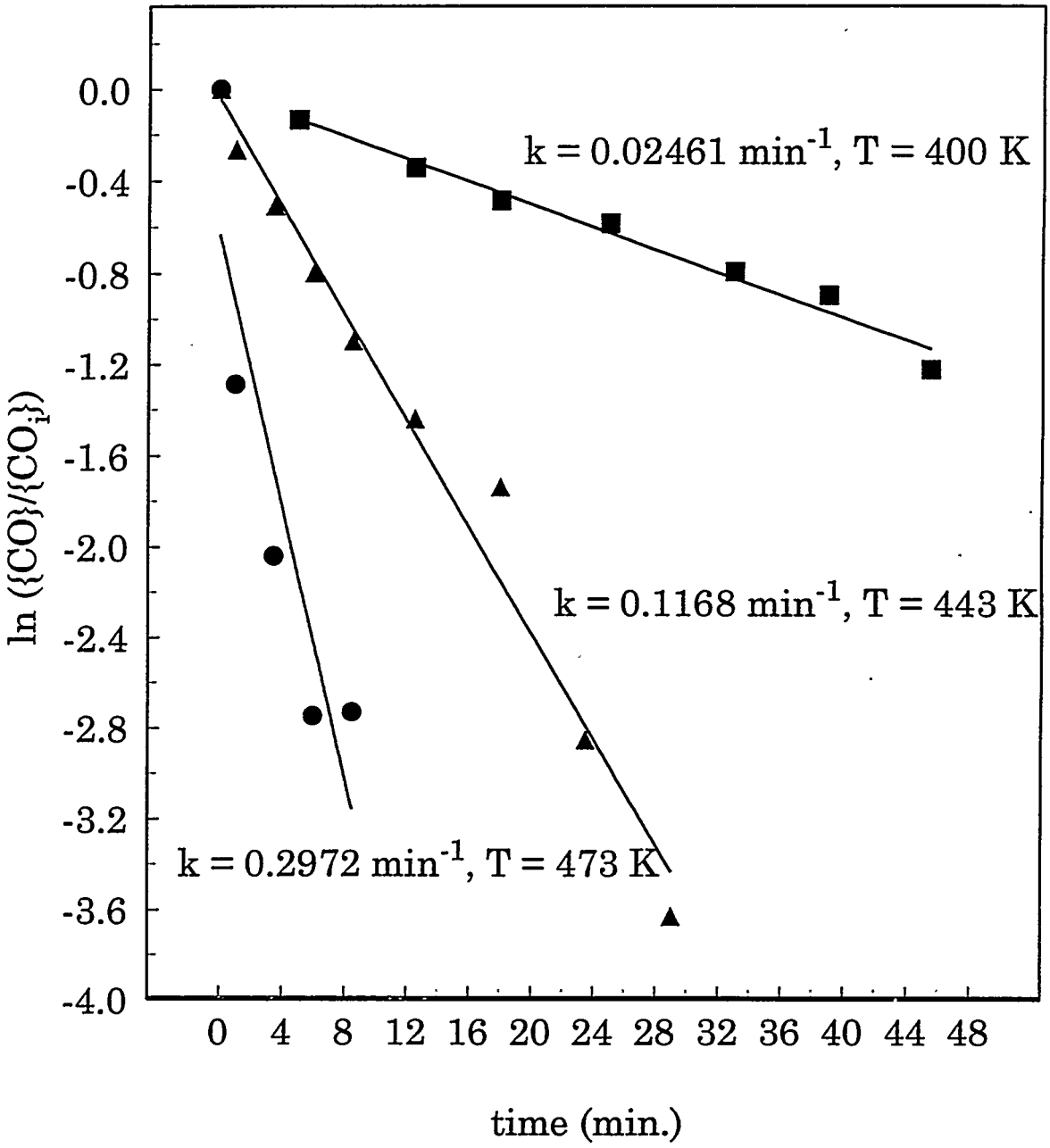

Figure E3. Kinetics of CO hydrogenation reaction on Ru/SiO_2

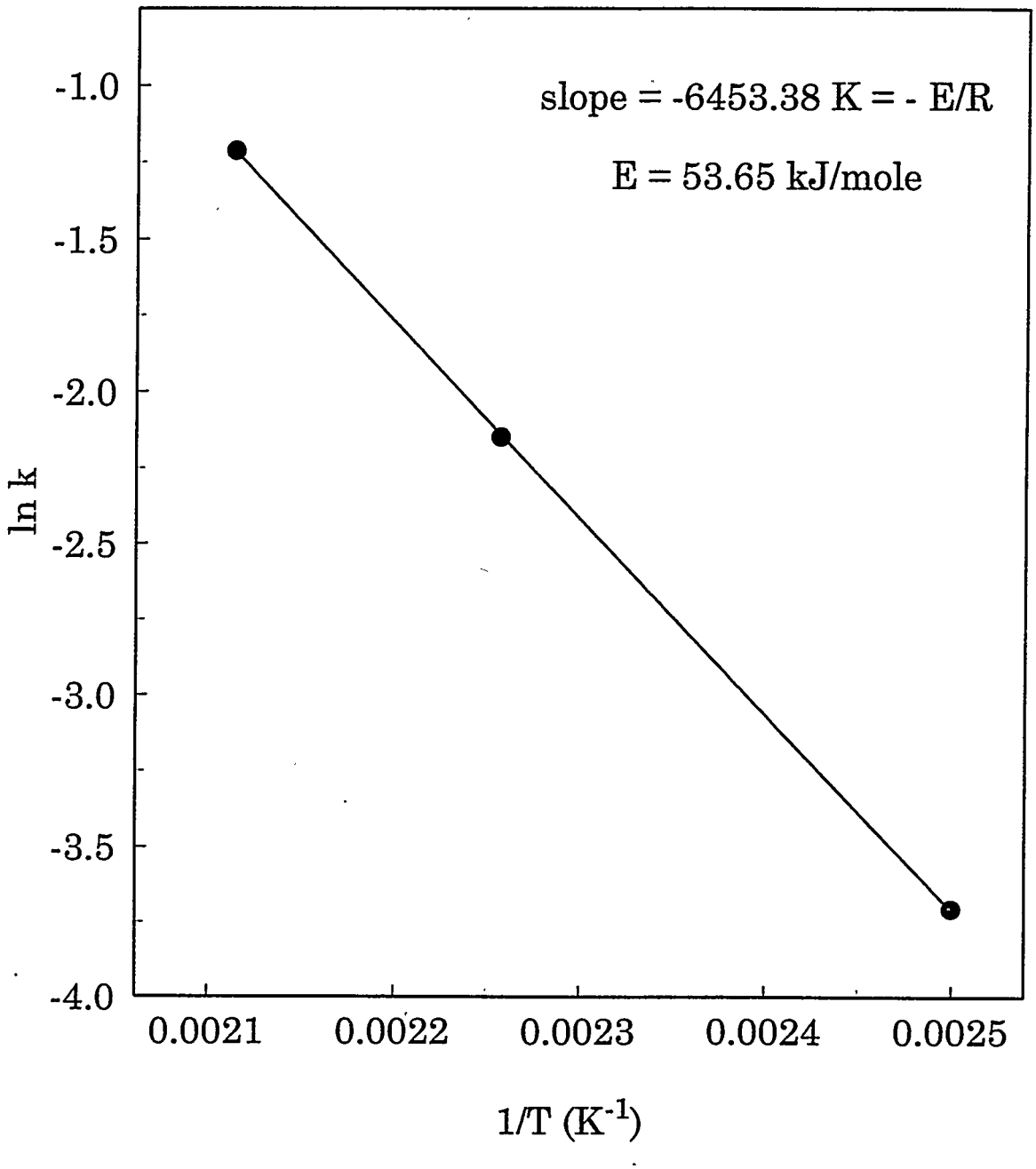

Figure E4. Arrhenius plot of rate constant versus temperature for CO hydrogenation over Ru/SiO_2

REFERENCES

1. Sinfelt, J. H., "Bimetallic Catalysts", Wiley, New York, (1983).
2. Satterfield, C. N., "Heterogeneous Catalysis in Industrial Practice", McGraw Hill Inc., New York, (1991).
3. van Delft, F. C. M. J. M., Niewenhuys, B. E., Siera, J., and Wolf, R. M., ISIJ International, 29(7), 550 (1989).
4. Burton, J. J., and Garten, R. L., "Advanced Materials in Catalysis", Academic Press, New York (1977).
5. Williams, F. L. and Nelson, G. C., Appl. Surf. Sci., 3, 409 (1979).
6. Holloway, P. H. and Williams, F. L., Appl. Surf. Sci., 3, 409 (1979).
7. van Langeveld, A. D. and Niemantsverdriet, J. W., Surf. Sci., 10, 1 (1982).
8. van Delft, F. C. M. J. M., Siera, J. and Niewenhuys, B. E., Surf. Sci., 208, 365 (1989).
9. Beck, D. D., DiMaggio, C. L.,and Fisher, G. B., Surf. Sci., 297, 293 (1993).
10. Beck, D. D., DiMaggio, C. L.,and Fisher, G. B., Surf. Sci., 297, 303 (1993).
11. Williamson, B. E., Gandhi, H. S., Wynblatt, P., Truex, T. J., and Ku, R. C., AIChE Symposium Ser., 76(201), 212 (1980).
12. Miura, H., and Gonzalez, R. D., J. Catal., 74, 216 (1982).
13. Miura, H., and Gonzalez, R. D., J. Phys. Chem., 86, 1577 (1982).
14. Miura, H., and Gonzalez, R. D., J. Phys. E (Sci. Instr.), 15, 373 (1982).

15. Miura, H., Suzuki, T., Ushikuko, Y., Sugiyama, K., Maatsuda, T. and Gonzalez, R. D., J. Catal., 85, 331 (1984).

16. Wang, T. and Schmidt, L. D., J. Catal., 71, 411 (1981).

17. Wu , X., Gerstein, B. C., and King, T. S., J. Catal., 121, 271 (1990).

18. Wang Z., Ansermet, J.-P., Slichter, C. P., and Sinfelt, J. H., J. Chem. Soc. Faraday Trans. I, 84(11), 3785 (1988).

19. Engelke, F., Vincent, R., King, T. S., and Pruski, M., J. Chem. Phys., 101(9), 7262 (1994).

20. Strohl, J. K., and King, T. S., J. Catal., 116, 540 (1989).

21. Wu , X., Gerstein, B. C., and King, T. S., J. Catal., 123, 43 (1990).

22. Uner, D. O., Pruski, M., Gerstein, B. C., and King, T. S., J. Catal., 156, 60 (1995).

23. Gibbs, J. W., "Collected Works", Vol. 1, Yale University Press, New Haven, CT (1948).

24. Butler, J. A. V., Proc. R. Soc. London, 135, 348 (1932).

25. Schuchowitzky, A., Acta Physicochim., URSS, 19(2-3), 176 (1944).

26. Guggenheim, E. A., Trans. Faraday Soc., 41, 150 (1945).

27. Defay, R., and Prigogine, I., Trans. Faraday Soc., 46, 199 (1950).

28. Schoeb, A. M., Raeker, T. J., Yang, L., Wu, X., King, T. S., and DePristo, A. E., Surf. Sci., 278, L125 (1992).

29. Ahmad, M., and Tsong, T. T., J. Vac. Sci. Technol. A, 3(3), 806 (1985).

30. Wolf, R. M., Siera, J., van Delft, F. C. M. J. M., and Niewenhuys, B. E., Faraday Discuss. Chem. Soc., 87, 275 (1990).

31. Zhu, Y. and Schmidt, L. D., Surf. Sci., 129, 107 (1983).

32. Oh, S. H., and Carpenter, J. E., J. Catal., 98, 178 (1986).

33. Wang, Z., Ph. D. Dissertation, Dept. of Physics, Univ. of Illinois at Urbana Champaign (1987).

34. Wu, X., Gerstein, B. C., and King, T. S., J. Catal., 123, 43 (1990).

35. Smale, M. W., and King, T. S., J. Catal., 119, 441 (1989).

36. Schick, M., Ceballos, G., Pelzer, Th., Rangelov, G., Stober, J., and Wandelt, K., Surf. Sci., 307, 582 (1994).

37. Rodriguez, J., Surf. Sci., 296, 149 (1993).

38. Bernasek, S. L., and Somorjai, G. A., J. Chem. Phys., 62(8), 3149 (1975).

39. Bhatia S., Engelke, F., Pruski, M., and King, T. S., Catalysis Today, 21, 129 (1994).

ACKNOWLEDGMENTS

I would like to express my gratitude towards Dr. Terry King for his guidance and support throughout my academic career at Iowa State University. I would also like to thank Dr. Marek Pruski for sharing his insight and knowledge of NMR spectroscopy with me. I also wish to thank Dr. Deniz Uner and Dr. Frank Engelke for useful discussions and suggestions regarding my research work. My thanks are also due to the past and present students of Dr. King and Dr. Gerstein, who provided enjoyable and helpful work environment. Last but most importantly, I would like to thank my parents and my brother Rajesh and sister-in-law Pratima for their moral support and encouragement during my pursuit of the doctoral degree.

This work was performed at Ames Laboratory under the Contract No. W-7405-Eng-82 with the U. S. Department of Energy. The United States government has assigned the DOE Report number IS-T 1794 to this thesis.